Pharmaceutical Sciences Asia

Pharm Sci Asia 2026; 53(3), 344-367

DOI:10.29090/psa.2026.03.26.9167

Research Article

Nanoparticle-based dual-triggered colon-targeted 5-fluorouracil tablets: A quality-by-design approach for improved colorectal cancer therapy

Yash Dipakkumar Dudhwala [1,2*], Dhiren Prafulbhai Shah [3*], Devesh Umesh Kapoor [4,5], Riya Kalpesh Mehta [2], Vinod Devchanbhai Ramani [3]

[1] Gujarat technological University, Chandkheda, Ahmedabad, Gujarat, Pin-382424, India
[2] Shree Naranjibhai Lalbhai Patel College of Pharmacy, Umrakh – 394345, Gujarat, India
[3] C. K. Pithawalla Institute of Pharmaceutical Science and Research, Surat- 395007, Gujarat, India
[4] Dr. Dayaram Patel Pharmacy College, Bardoli-394601, Gujarat, India
[5] Centre for Research Impact & Outcome, Chitkara College of Pharmacy, Chitkara University, Rajpura, 140401, Punjab, India

ABSTRACT

Colorectal cancer (CRC) ranks among the top three most commonly diagnosed cancers worldwide and remains a leading cause of cancer-related deaths, accounting for nearly 10% of global cancer incidence. Despite advances in treatment, chemotherapy with 5-fluorouracil (5-FU) continues to be a mainstay; however, its rapid systemic clearance, limited tumor selectivity, and gastrointestinal toxicity significantly compromise therapeutic efficacy. To address these limitations, this study aimed to design and optimize a pH- and microflora-activated colon-targeted tablet containing 5-FU-loaded, folic acid-conjugated chitosan (FA-CS) nanoparticles for site-specific CRC therapy. The nanoparticles were prepared using ionic gelation with sodium tripolyphosphate (STPP) as a cross-linking agent and optimized through a Box–Behnken design (BBD). The optimized batch containing 0.45 mg/mL folic acid-conjugated chitosan, 0.50 mg/mL STPP, and 10.0 mg 5-FU exhibited a particle size of 232.5 nm, a polydispersity index of 0.307, and an entrapment efficiency of 81.3%. The nanoparticles were compressed into core tablets and sequentially coated with Eudragit E100, hydroxypropyl methylcellulose K15M (HPMC K15M), and Eudragit S100 to achieve delayed colon-targeted release. *In vitro* studies showed minimal drug release in gastric and intestinal media, followed by nearly complete release (approximately 96%) under simulated colonic conditions. The formulation also remained stable under accelerated conditions, supporting its potential for CRC therapy.

Keywords:
5-Fluorouracil; Chitosan nanoparticles; pH-responsive delivery; Box–Behnken design; Colorectal cancer

1. INTRODUCTION

Colorectal cancer (CRC) remains a major cause of cancer illness and death worldwide. The rising burden is attributed to various factors, including urbanization, shifting toward high-fat and low-fiber diets, sedentary habits, and inherited risk. In India, the ranks based on surveillance data from the Indian Council of Medical Research are as follows: colon cancer ranks eighth and rectal cancer ninth among men, while colon cancer is ninth among women [1]. Clinically, CRC is a cause for concern as it has a propensity for rapid progression and early metastasis, allowing malignant cells to seed into distant organs. Better screening and more options for therapy notwithstanding, outcomes in advanced disease are still poor. This gap keeps the focus on treatment strategies that deliver drugs precisely to the tumor site and spare healthy tissues [2].

***Corresponding author:**
* Yash Dipakkumar Dudhwala Email: yashdudhwala70@gmail.com
* Dhiren Prafulbhai Shah Email: dhirenpshah1@gmail.com

5-Fluorouracil (5-FU) has been the chemotherapeutic backbone for CRC management for over six decades. It is a pyrimidine analogue exhibiting its antineoplastic action through the inhibition of thymidylate synthase, and its metabolites (fluorodeoxyuridine triphosphate and fluorouridine triphosphate) are incorporated into DNA and RNA, disrupting nucleic acid synthesis with resultant apoptosis in rapidly dividing cells [3]. However, conventional 5-FU therapy suffers from severe drawbacks represented by rapid metabolic degradation by dihydropyridine dehydrogenase in the liver and gastrointestinal tract, short plasma half-life, poor selectivity toward tumor tissue, and systemic toxicities including mucositis, diarrhea, and myelosuppression. These pharmacokinetic limitations result in sub-therapeutic concentrations at the colonic tumor site and significant off-target adverse effects, and repeated high doses and continuous infusion protocols are required, compromising patient compliance [4].

Therefore, to prevail over these deficiencies, colon-specific drug delivery presents an attractive approach for the localized treatment of CRC. Colon targeting of 5-FU might improve its local cytotoxic effect and reduce systemic exposure and related upper gastrointestinal toxicity [5]. Conventional gastro-resistant enteric-coated tablets, designed to resist gastric acid, have had partial success but frequently fail in ensuring precise colonic release, given that premature drug liberation may occur at the distal small intestine, where the pH is already considerably above the polymer threshold [6]. Hence, a dual-triggered approach may afford superior specificity by incorporating both pH-dependent and microflora-activated mechanisms. The human colon is home to a dense population of bacteria (~10^{11}–10^{12} CFU/mL) capable of producing different enzymes, including β-galactosidase, azoreductase, and glycosidase, which can degrade polysaccharide-based carriers. Incorporation of microflora-degradable polymers, particularly carbohydrate derivatives such as chitosan, enables selective colon drug release in the colonic lumen, where these enzymes are highly abundant. In addition, enzymatic degradation of polysaccharide-based carriers by colonic microflora can loosen the polymer matrix, increase porosity, and promote drug diffusion, thereby supporting site-specific release in the colon [7].

While pH- and microflora-responsive systems improve site-specificity, achieving intracellular tumor targeting remains a formidable challenge. The heterogeneous tumor microenvironment, multidrug resistance mechanisms, and overexpression of efflux transporters such as P-glycoprotein limit the effective uptake of cytotoxic drugs [8]. Nanoparticle-based delivery systems provide a versatile platform to address these barriers. Owing to their nanoscale dimensions (10–500 nm), nanoparticles can exploit the enhanced permeability and retention (EPR) effect, enabling passive accumulation within tumor tissue through leaky vasculature and impaired lymphatic drainage [9]. Furthermore, their surface chemistry can be engineered for active targeting by attaching ligands that recognize receptors overexpressed on cancer cells. Among the various biopolymers explored, chitosan, a cationic polysaccharide derived from chitin, is particularly appealing due to its biocompatibility, biodegradability, mucoadhesive nature, and ability to form polyelectrolyte complexes with anionic cross-linkers such as sodium tripolyphosphate (STPP) via ionic gelation [10].

Folic acid, a water-soluble vitamin (vitamin B9), is one of the most employed targeting ligands in attempts to enhance tumor selectivity. The folate receptor-α (FR-α) is overexpressed on the surface of many epithelial tumors, including colorectal, ovarian, and breast carcinomas, while its expression in normal tissues remains minimal [11]. Ligation of folic acid to the surface of polymeric nanoparticles promotes receptor-mediated endocytosis and hence increases intracellular accumulation of the therapeutic payload [12]. Indeed, a series of reports has demonstrated the significant improvement in cytotoxicity of various anticancer agents by folate-functionalized chitosan nanoparticles due to improved cellular internalization and prolonged residence time in tumor tissue. Finally, the folic acid-conjugated chitosan (FA-CS) nanoparticles system combines in a synergistic way passive (EPR-based) and active (ligand-mediated) targeting mechanisms [13].

In this regard, the current study aimed at the development and optimization of 5-FU-loaded FA-CS (5-FU-FA-CS) nanoparticles and their subsequent incorporation into a colon-targeted tablet with pH- and microflora-responsive release characteristics. For formulation and optimization of the 5-FU-FA-CS nanoparticles, a Box-Behnken design-based Quality-by-Design (QbD) approach was employed to evaluate the impact of critical formulation variables, such as polymer concentration, crosslinker level, and 5-FU loading, on particle size, polydispersity index, and entrapment efficiency. Subsequently, the optimized 5-FU-FA-CS nanoparticles were incorporated into core tablets, which were coated sequentially with Eudragit E100, hydroxypropyl methylcellulose K15M (HPMC K15M), and Eudragit S100 in a multilayered manner to obtain delayed release in the lower gastrointestinal tract. Eudragit S100 served as the outer pH-dependent enteric layer, HPMC K15M acted as an intermediate swellable barrier, and Eudragit E100 functioned as an inner release-modulating layer. This polymer combination was selected to minimize premature drug release in the upper gastrointestinal tract and promote drug release in the colon in conjunction with the microflora-responsive matrix [14].

Therefore, this study aimed to develop a dual-triggered, ligand-targeted nanocarrier system that can selectively deliver 5-FU to the colonic tumor site. This approach, by integrating polymer science and nanotechnology along with the principles of QbD, has the potential to overcome the pharmacokinetic limitations of conventional 5-FU therapy, enhance local drug amount at the tumor microenvironment, and reduce systemic toxicity. Such a strategy will exemplify the potential of bio nanotechnology in oncology and provide a rationale for designing oral nanomedicines that can transform CRC chemotherapy [15].

2. MATERIALS AND METHODS

2.1. Materials

5-FU was obtained as a generous gift sample from Globela Pharma PVT. LTD, Surat, India. Chitosan (medium molecular weight, 75–85 % deacetylated) was procured from Balaji Drugs, Surat. Folic acid, STPP, Eudragit E100, Eudragit S100, HPMC K15M, and all analytical-grade solvents (methanol, ethanol, acetone, acetic acid, dimethyl sulfoxide (DMSO)) were purchased from Loba Chemie PVT. LTD., Mumbai, India. All reagents and chemicals were of analytical or pharmaceutical grade and used as received. Deionized distilled water was employed throughout the study.

2.2. Development of folic acid-conjugated chitosan polymer

The folic acid-conjugated chitosan (FA–CS) was synthesized via a carbodiimide-mediated coupling reaction using 1-ethyl-3-(3-dimethylaminopropyl) carbodiimide (EDC) as an activating agent. Initially, folic acid and EDC were dissolved in 15 mL of anhydrous DMSO in a molar ratio of 2:5, and the solution was stirred at room temperature until complete dissolution was achieved. The resulting activated folic acid solution was added dropwise to a 10 mg/mL chitosan solution prepared in 1% (v/v) acetic acid (pH 4.7), followed by continuous stirring at room temperature in the dark for 16 h to promote amide bond formation between folic acid and the amino groups of chitosan [13, 16].

Upon completion of the reaction, the pH of the mixture was carefully adjusted to 9.0 using 1.0 M sodium hydroxide to precipitate the conjugate. To collect the FA-CS conjugate, the suspension was centrifuged at 2500 rpm for 10 min. The resulting precipitate was further purified by dialysis: against phosphate-buffered saline (PBS, pH 7.4) for the first 48 h to remove unreacted folic acid and residual reagents, then against deionized water for 96 h. The obtained purified conjugate was freeze-dried and appeared as a pale-yellow sponge-like product. After that, the product was stored in a desiccator at room temperature for further characterization [17].

2.2.1. Characterization of folic acid-conjugated chitosan by Fourier-transform infrared spectroscopy

The folic acid-conjugated chitosan (FA-CS) conjugate was characterized by Fourier-transform infrared spectroscopy (FTIR) to evaluate functional group changes associated with conjugation. Fresh FTIR spectra of chitosan, folic acid, and FA-CS conjugate were recorded for the present study using a Cary 630 FTIR spectrometer (Agilent Technologies, USA) over the range of 4000-650 cm^{-1}. Each spectrum was recorded with 32 sample scans and 32 background scans at a resolution of 8 cm^{-1}. The important diagnostic peaks were used to compare the spectral features of chitosan, folic acid, and FA-CS conjugate [18].

2.3. Preparation of 5-fluorouracil-loaded folic acid-conjugated chitosan nanoparticles

The 5-FU-FA–CS nanoparticles were formulated via the ionic gelation technique, based on the electrostatic interaction between positively charged amino groups of chitosan and negatively charged phosphate groups of STPP [19]. Various concentrations of the FA–CS conjugates were prepared according to the experimental design by dissolving a predetermined amount of the lyophilized FA–CS conjugate sponge in 10 mL of 0.01 M acetic acid solution, adjusted to pH 4.0 [17]. Separately, different concentrations of STPP were prepared by dissolving the appropriate amount of STPP in distilled water, and the pH of this solution was adjusted to 2.0 using 1.0 M HCl. The required amount of 5-FU was then added to the STPP solution and stirred gently until completely dissolved [16].

The STPP–drug solution (2 mL) was added dropwise into the FA–CS solution (5 mL) at a controlled flow rate of 0.5 mL/min, under continuous magnetic stirring at 500 rpm at room temperature. The spontaneous ionic crosslinking reaction between the oppositely charged species led to the formation of a uniform suspension of nanoparticles.

The resulting nanoparticle dispersion was centrifuged at 25,000 rpm for 3 min to separate the nanoparticles, and the collected pellet was washed with deionized water to remove unreacted residues [20]. The purified nanoparticles were immediately frozen at −80 °C for 12 h (Deep Freezer, SU105UE, Stirling Ultracold, USA) and then lyophilized at −40 °C for 48 h using a freeze dryer (Model MSW-137, Macro Scientific Works, Delhi). The obtained dry 5-FU-FA–CS nanoparticles were stored in a desiccator at 4 °C until further characterization and formulation into colon-targeted tablets.

2.3.1. Experimental design and optimization

QbD is an investigative strategy that applies risk-based science and techniques to refine the design and handling of products and processes. QbD incorporates critical quality attributes (CQAs) and critical process parameters (CPPs) [21, 22]. Experimental design and optimization were performed using Design-Expert ®v13.0.5 (Stat-Ease Inc., Minneapolis, MN, USA). Box-Behnken design: in 14 runs with two center points, the three important factors were examined at three levels (-1, 0 and +1). FA-CS concentration (mg/mL), STPP concentration (mg/mL) and drug amount (mg) was taken as independent variables and particle size (Y_1), polydispersity index (PDI, Y_2), and entrapment efficiency (%EE, Y_3) were the responses.

2.3.2. Identification of quality target product profile (QTPP), critical quality attributes (CQAs) and critical process parameters (CPPs)

QbD principles defined the QTPP of the colon-targeted 5-FU formulation, including the intended route of administration (oral), dosage form (pH-microflora-activated coated tablet), site-specific drug release in the colon, acceptable mechanical strength, and chemical and physical stability over shelf-life. Potential CQAs were identified based on the QTPP: nanoparticle-related attributes such as particle size, PDI, zeta potential, and entrapment efficiency; tablet attributes such as hardness, friability, coat integrity, and drug content; and *in vitro* performance parameters, viz., lag time in gastric/small intestinal media and ≥90% release in simulated colonic conditions [23]. The formulation-level CMAs, FA–CS concentration, STPP concentration, 5-FU loading, and lactulose/microcrystalline cellulose (MCC) ratio, and process-level CPPs, namely, stirring speed, STPP addition rate, pH of polymer and crosslinker solutions, and coating weight gain, were identified to consistently achieve these CQAs for subsequent risk assessment and Design of Experiment (DoE) studies [24].

2.3.3. Design of Experiment (DoE) approach for optimization study for nanoparticle formulation using Box Behnken design

We first conducted one-factor-at-a-time (OFAT) trials to bracket feasible concentrations of each component while keeping an eye on nanoparticle formation and preventing macroscopic aggregation, guided by the literature and our pilot work. FA-CS concentration varied from 0.1 to 0.5 mg/mL, STPP concentration from 0.5 to 1.0 mg/mL, and drug amount from 10 to 25 mg. These experiments established a stable range of conditions wherein ionic gelation consistently produced colloidally stable suspensions appropriate for formal optimization [25].

A three-factor, three-level Box–Behnken Design was then employed to model and optimize the effects of FA-CS concentration (X_1), STPP concentration (X_2), and drug amount (X_3) on the CQAs: particle size (Y_1), PDI (Y_2), and %EE (Y_3). Factor levels were coded at −1, 0, and +1 corresponding, respectively, to 0.1, 0.3, and 0.5 mg/mL for FA-CS concentration; 0.5, 0.75, and 1.0 mg/mL for STPP concentration; and 10, 17.5, and 25 mg for drug amount the design comprised 14 experimental runs (12 factorial points and 2 replicates at the center point) executed in randomized order to mitigate systematic bias. Responses were fitted to a second-order polynomial model of the form:

$$Y=\beta_0 + \Sigma\beta_i X_i + \Sigma\beta_{ii} X_i^2 + \Sigma\beta_{ij} X_i X_j$$

where X_i are coded variables. Model adequacy was assessed by analysis of variance (ANOVA), coefficient of determination (R^2 and adjusted R^2), lack-of-fit testing against pooled pure error from center points, and standard diagnostic plots (normal probability of residuals, residuals vs. predicted). Influence and interaction effects were visualized through perturbation and response-surface/contour plots [26].

Using a composite desirability function, optimization was carried out with the objectives of minimizing Y_1 (size) and Y_2 (PDI) and maximizing Y_3 (%EE), subject to the screening study's feasibility constraints (no visible aggregation; Z-average < 200 nm; PDI ≤ 0.30 and maximum %EE) [27]. In a confirmatory batch made at the recommended factor settings, the model's predicted global optimum was experimentally confirmed.

2.4. Characterization of optimized 5-fluorouracil-loaded folic acid-conjugated chitosan nanoparticles

2.4.1. Particle size, polydispersity index (PDI), and zeta potential

The size distribution, mean hydrodynamic diameter (Particle size), and surface charge of the optimized 5-FU-FA–CS nanoparticles were investigated by dynamic light scattering (DLS) using Malvern Zetasizer [Zetasizer Ultra, Malvern Panalytical, Malvern, UK]. A small amount of lyophilized nanoparticles was dispersed in double-distilled water and slightly sonicated to avoid aggregation or rupture of the nanostructure. Thereafter, the dispersion was transferred to a disposable polystyrene cuvette and analyzed at 25 ± 1 °C with a detection angle of 173° (backscatter mode). The Z-average particle size and PDI were automatically calculated by the instrument. In the case of zeta potential measurements, the same diluted

dispersion was loaded into a folded capillary cell, and electrophoretic mobility was determined; All the measurements were carried out in triplicate and reported as mean ± SD [28].

2.4.2. Scanning electron microscopy (SEM)

To examine the morphology the optimized nanoparticles, their surface and shape were observed under a scanning electron microscope (JSM-6010LA; JEOL, Tokyo, Japan). A small amount of the freeze-dried powder was placed on an aluminum stub, fixed with carbon tape, and coated with a thin layer of gold to make it conductive. The sample was then viewed at an accelerating voltage of about 10–15 kV. The SEM images were used to check whether the particles were spherical, smooth, and discrete, or whether they showed any signs of aggregation. A smooth and uniform surface was considered desirable because it supports good redispersion and is typically associated with controlled ionic-gelation–type chitosan nanoparticles [29].

2.4.3. % Entrapment efficiency

The optimized nanoparticles were collected from the supernatant by spinning it in a cooling centrifuge (Model C-24BL, REMI Instruments Ltd., Mumbai, India) at 12000 rpm for half an hour, after which the supernatant was taken out. To find the concentration of the free drug in the supernatant, it was diluted in water, and the absorbance was measured at 266 nm with a UV-Visible spectrophotometer (UV-1900i, Shimadzu, Kyoto, Japan), using water as a blank. Percentage entrapment was then calculated using below equation (1) [24].

Equation 1

$$\%EE = \frac{\text{Amount of total drug - Amount of free drug in supernant}}{\text{Amount of total drug}} \times 100$$

2.4.4. Drug content

To determine the drug content within the formulated nanoparticles, a 10 mg sample was mixed with 50 mL of methanol and subjected to sonication for 20 minutes to ensure complete breakdown of the nanoparticles. After sonication, 1 mL of the resulting solution was further diluted to 50 mL with methanol. The absorbance of the final diluted solution was measured at 266 nm using a UV-Visible spectrophotometer (UV-1900i, Shimadzu, Kyoto, Japan). The Drug Amount was calculated from the calibration curve using the regression equation, $y = 0.0192x - 0.0244$ ($R^2 = 0.9993$). The percentage drug content was then calculated using Equation (2) [30].

Equation 2

$$\%\text{Drug Content} = \frac{\text{Amount of drug present in nanoparticles}}{\text{Weight of nanoparticles taken}} \times 100$$

2.4.5. % Yield

The production yield of the optimized 5-FU-FA–CS nanoparticles was calculated to understand how efficiently the ionic-gelation process converted the input materials into the final dried product. After lyophilization, the total weight of the dried nanoparticles was recorded and compared with the total weight of all solids initially used in the batch (FA–CS, STPP, and 5-FU). The % yield of optimized batch of nanoparticles was calculated using to the following equation (3) [17].

Equation 3

$$\%\ \text{Yield} = \frac{\text{Weight of obtained nanoparticles}}{\text{Weight of drug} + \text{Weight of Stabilizer}} \times 100$$

2.4.6. In vitro drug release studies for optimized nanoparticles

Release of the drug from the optimized nanoparticles *in vitro* was done in two pH environments to support the concept of targeting. It is a known fact that solid tumors and inflamed colonic tissues have a slightly acidic micro-environment compared to normal tissues. Hence, the release of the drug was investigated in PBS at pH 5.0, simulating the acidic environment of the tumor or inflamed colon tissue, and at pH 7.4, simulating the normal physiological environment [31, 32]. The investigation was done with the aim of evaluating the ability of the FA-CS system to control the release of the drug in accordance with the pH of the environment.

A known amount of nanoparticle dispersion, equivalent to a fixed dose of 5-FU, was placed in a pre-soaked dialysis bag (MWCO 12 kDa), and the bag was immersed in 20 mL of the respective buffer maintained at 37 ± 0.5 °C in a shaking water bath (≈120-130 rpm). The release study was continued for a total period of 8 h. At predetermined time intervals of 0.5, 1, 2, 3, 4, 5, 6, 7, and 8 h, 1 mL of the medium was withdrawn, analyzed at 266 nm using a UV-Visible spectrophotometer (UV-1900i, Shimadzu, Kyoto, Japan), and immediately replaced with an equal volume of fresh, pre-warmed buffer to maintain sink conditions. The cumulative percentage of drug released was calculated with volume correction. The two release profiles obtained at pH 5.0 and pH 7.4 were then compared to evaluate whether the formulation showed preferential release under acidic conditions [33].

2.4.7. Release kinetics and mechanism analysis

After getting the *in vitro* release data at pH 5.0 and pH 7.4, we examined the pattern of 5-FU release from the nanoparticles. The percentage drug released at each time point was entered in Excel and fitted to the usual release models: zero order, first order, Higuchi, and Korsmeyer–Peppas. For the Peppas model, only the initial part of the curve (up to about 60% release) was used, because that part best reflects the real mechanism. For each model, the correlation coefficient (R^2) was calculated and the model with the higher R^2 was taken as the most suitable one. In the Peppas model, the release exponent (n) was also noted, since it helps to tell whether the drug mainly came out by simple diffusion through the chitosan network or by a mixed process of diffusion and polymer relaxation. This small analysis was useful to compare the behavior of the nanoparticles at the two pH values and to see whether the formulation was closer to a diffusion-controlled system or to an erosion-type system 34.

2.4.8. Ex vivo drug release studies for optimized nanoparticles

An *ex vivo* study of the release/permeation of the optimized 5-FU-FA-CS nanoparticles was conducted by using the non-everted rat colonic sac method. The study was approved by the Institutional Animal Ethics Committee of Shree Naranjibhai Lalbhai Patel College of Pharmacy, India (approval no. CCDES/SNLPCP/IAEC/26/01/190). Adult male Wistar rats weighing between 180-220 g were chosen for the study. The rats were fasted overnight but allowed free access to water. They were sacrificed under deep anesthesia, and the excised colon was immediately placed in ice-cold oxygenated Krebs-Ringer phosphate buffer (KRPB), pH 7.4. The colon was cleaned by removing fat and adhering mesenteries, while the circular and longitudinal muscles were gently stripped, followed by the preparation of 6-cm long segments of the rat colon, which was then rinsed with oxygenated normal saline (0.9% w/v NaCl).

The open end of each segment of the colon was ligated using surgical thread. The sac was then filled with 2 mL of the 5-FU-FA-CS nanoparticles dispersion containing 50 mg of 5-FU using a blunt needle. The other end of the sac was also ligated. This resulted in a closed non-everted sac of about 6 cm in length. Each sac was then placed in a conical flask containing 50 mL of oxygenated KRPB (pH 7.4). The flasks were maintained at 37 ± 1 °C in a shaking water bath at 50 rpm.

At predetermined time intervals of 0.5, 1, 2, 4, 6, 8, 10, and 12 h, 2 mL of the samples were withdrawn from the external medium and immediately replaced with the same volume of fresh pre-warmed buffer solution to maintain the sink conditions. The samples were then analyzed for 5-FU using the using the validated HPLC method. HPLC analysis was chosen for the *ex vivo* samples to avoid any interference from the biological matrix constituents of the samples and to specifically quantify the 5-FU released/permeated into the medium. A parallel experiment was conducted with blank FA-CS nanoparticles to obtain the background response, which was subtracted from the test response.

The cumulative 5-FU released/permeated into the external medium was calculated as a function of time. The results were further analyzed using the commonly employed kinetic models such as zero-order, first-order, Higuchi, and Korsmeyer-Peppas models to interpret the release/permeation behavior of 5-FU-FA-CS nanoparticles through the colonic membrane.

2.5. Preparation of core tablets containing 5-fluorouracil-loaded folic acid-conjugated chitosan nanoparticles

The optimized 5-FU-FA–CS nanoparticles were converted into an oral solid dosage form to enable colonic delivery. Core tablets were prepared by direct compression by rotary tablet compression machine (Mini Press I, Rimek, Ahmedabad, India), since this method avoids heat and solvent and is therefore suitable for nanoparticle-based systems. A quantity of nanoparticle powder equivalent to 100 mg of 5-FU (calculated from the drug content of the optimized batch) was accurately weighed and mixed with the remaining tablet excipients in a clean polybag for about 10 minutes to ensure uniform distribution. Along with the nanoparticles, lactulose was added as a microflora-degradable component and MCC was used as the main filler and to adjust the tablet weight. Talc and magnesium stearate were added at the end as glidant and lubricant, respectively illustrated in Table 1 [35].

The final blend was compressed on a rotary tablet compression machine using a 9 mm round, flat punch to obtain tablets of about 250 mg target weight. Three formulations were prepared by varying the proportion of lactulose and MCC so that the effect of the degradable carbohydrate on the later colonic release could be studied. The freshly compressed core tablets were stored in tightly closed containers until further coating.

2.6. Evaluation of core tablets containing 5-fluorouracil-loaded folic acid-conjugated chitosan nanoparticles

Core tablets were evaluated for thickness, hardness, friability, weight variation, and assay of drug

Table 1. Composition of core tablets containing 5-FU-FA–CS nanoparticles.

Ingredients	F1 (mg)	F2 (mg)	F3 (mg)
5-FU-FA–CS nanoparticles	equivalent to 100 mg 5-FU		
Lactulose	40	60	80
Microcrystalline cellulose (MCC)	87.75	67.75	47.75
Talc	5	5	5
Magnesium stearate	5	5	5
Total tablet weight (mg)	**250**	**250**	**250**
Punch: 9.0 mm flat, round punch on a rotary tablet compression machine.			

content according to the Indian Pharmacopoeia 2018. Each test was performed in triplicate using standard instruments. The results indicated that all tablet batches were stored in tightly closed containers until further coating.

2.7. Coating of core tablets containing 5-fluorouracil-loaded folic acid-conjugated chitosan nanoparticles

To make the tablets release 5-FU only after reaching the colon, they were coated in a multilayer structure composed of different polymers applied in a defined sequence. First, three coats of Eudragit E100 (12% w/v) were applied as the inner release-modulating layer adjacent to the core. Next, a thin HPMC K15M (2% w/v) barrier layer was added to separate the two pH-sensitive coats and to prevent any possible interaction between them [37]. Lastly, two layers of Eudragit S100 (10% w/v) solution were used as the pH-dependent protective layer, allowing the tablet to withstand the acidic environment of the stomach and the upper part of the intestine while disintegrating in the higher pH of the colon region. Thus, in the multilayered coating approach, Eudragit S100 was used as the primary pH-dependent protective layer, whereas HPMC K15M was the intermediate layer, and Eudragit E100 was the inner layer of the release modifier rather than the acid-resistant coating layer. Thus, the developed coating structure of the tablet includes the core tablet, followed by three layers of Eudragit E100, one layer of HPMC K15M, and two layers of Eudragit S100.

The coating solutions were prepared with appropriate solvents. Eudragit E100 and S100 were prepared with isopropyl alcohol and acetone (1:1), whereas HPMC K15M was prepared with distilled water as the solvent. The coating operation was done using the dip-coating method. The tablets were allowed to air-dry for 20 minutes after each coating operation. They were then dried in a hot air oven at 40°C for 45 minutes. The gain in the weight of the tablets was observed after each operation to ensure uniform layer formation. The tablets were stored in tightly closed containers at room temperature [38].

2.8. Coating integrity testing

The strength and continuity of the coated layers were checked to ensure that the tablets could withstand the different pH conditions of the gastrointestinal tract before releasing the drug in the colon. The test was performed on dummy tablets to optimize the number of coating layers required for Eudragit E100 and Eudragit S100 before finalizing the multilayer coating design, rather than after completion of each layer of the final multilayer-coated tablets [39].

For the Eudragit E100 coats, individually coated tablets were placed in PBS (pH 7.4) for 6 hours and then in PBS (pH 5.0) for 4 hours to check whether the layers remained intact or showed any swelling or rupture. Similarly, for the Eudragit S100 layer coats, individually coated tablets were exposed first to 0.1 N HCl (pH 1.2) for 2 hours and then transferred to PBS (pH 7.4) for another 6 hours [40]. The HPMC K15M layer was not separately optimized in this test, as it was used only as an intermediate barrier between the two Eudragit layers**.**

The integrity of the coating was visually observed at each stage. A tablet that remained intact (no cracks, swelling, or disintegration) during the simulated gastric and intestinal phases was considered to have a satisfactory coating. Based on these observations, three coats of Eudragit E100 and two coats of Eudragit S100 were selected for the final multilayer coating system.

2.9. Evaluation of coated tablets

The physical quality of the tablets, after coating, was verified to ensure that the process of coating did not affect them. The thickness, hardness, friability, weight uniformity, and appearance of the coated tablets were studied by following the procedures outlined in the Indian Pharmacopoeia 2018.

Thickness and diameter were measured by a vernier calliper, while the hardness of the tablet was tested by a tablet hardness tester. Friability was evaluated using a friabilator (Model: FT1020, Lab India Instruments Pvt. Ltd., Mumbai, Maharashtra, India) to assess the ability of coated tablets to withstand mechanical stress during handling. Weight uniformity tests were determined by measuring the weight of twenty tablets from each batch and calculating the mean ± SD. The coated tablet surface was also observed visually to confirm that it was smooth, uniform, and free from cracks or imperfections. All values were found to be within acceptable limits, confirming that the coated tablets possessed adequate strength and uniformity for further *in vitro* release studies [41].

2.9.1. In vitro drug release studies for coated tablets

The coated tablets were tested for drug release under conditions that mimic the pH changes along the gastrointestinal tract. The main goal was to confirm that the coating would stop the drug from coming out in the stomach and small intestine but allow it to release once it reached the colon.

The study was carried out using a USP type I dissolution test apparatus (Model TDT-08L Electrolab, Mumbai, India) at 37 ± 0.5 °C and 100 rpm**.** USP Apparatus I (basket method) was selected to ensure that the multilayer-coated tablets remained fully immersed and mechanically stable during sequential exposure to different dissolution media. This approach also helped minimize problems such as floating, sticking to the vessel bottom, or irregular movement during medium transfer, which could affect the release behavior of the coated tablets. Tablets were first kept in 0.1 N HCl (pH 1.2) for 2 hours to represent the stomach, then transferred to phosphate buffer pH 7.4 for 6 hours to simulate the small intestine. Finally, they were placed in phosphate buffer pH 6.8 containing β-galactosidase enzyme (120 IU) for 4 hours to represent the colon. At fixed time points, 5 mL of the sample was taken out, filtered, and checked for absorbance at 266 nm using a UV-Visible spectrophotometer (UV-1900i, Shimadzu, Kyoto, Japan). The same volume of fresh, warm buffer was added after every sampling to keep the volume constant. The percentage of drug released at each time point was calculated and plotted against time. This test helped to show that the coated tablets stayed intact in the upper parts of the gut and released 5-FU mainly in the colonic phase, confirming successful colon targeting [42].

2.10. Drug release kinetics for coated tablets

The data obtained from the *in vitro* drug release studies were further analyzed to understand how 5-FU was released from the coated tablets. The cumulative percentage of drug released at different time intervals was fitted to common kinetic models, including zero-order, first-order, Higuchi, and Korsmeyer–Peppas equations [43].

For the Peppas model, only the initial portion of the release curve (up to about 60%) was used to get a more accurate value of the release exponent (*n*). The correlation coefficient (R^2) for each model was calculated, and the model showing the highest R^2 value was considered to best describe the release pattern. The value of *n* was used to understand whether the release was mainly by simple diffusion, by erosion of the coating, or by a combination of both [44].

This kinetic study helped to explain how the tablet coating controlled the release of 5-FU and supported the colon-targeting mechanism seen in the dissolution test.

2.11. Stability studies

The stability of the optimized coated tablets was checked to make sure that the formulation remained unchanged during storage. The study was carried out according to ICH guidelines (Q1A R2) under accelerated conditions of 40 ± 2 °C temperature and 75 ± 5% relative humidity for one month. Samples were kept in aluminum foil pouches laminated with polyethylene to protect them from light and moisture. At the end of the study period, the tablets were evaluated for physical appearance, drug content, and *in vitro* drug release using the same methods as before [45].

The results were compared with the initial values, and the similarity factor (f_2) was calculated to see if the release profile had changed significantly. A similarity factor greater than 50 was considered acceptable, indicating that the formulation remained stable and retained its performance throughout the storage period [19].

3. RESULTS AND DISCUSSION

3.1. Characterization of folic acid-conjugated chitosan by Fourier-transform infrared (FTIR) spectroscopy

Folic acid-chitosan conjugation was assessed by using Fourier transform-infrared spectroscopy (FTIR). FTIR spectra were obtained for chitosan, folic acid, and folic acid-chitosan conjugate (FA-CS). Spectral changes were assessed in order to identify the functional groups present and their variations after conjugation.

For the case of chitosan, peaks around 3354 and 3287 cm^{-1} were found corresponding to the O-H and N-H stretching vibrations, respectively. Moreover, peaks around 2870 cm^{-1} corresponded to the C-H stretching vibrations. The peaks at 1640 and 1587 cm^{-1} corresponded to the amide I and N-H bending vibrations, respectively.

Further, peaks at 1420, 1375, 1058, and 1025 cm^{-1} corresponded to the CH_2 bending and C-O/C-O-C stretching vibrations, respectively (Figure 1A) [46].

For the folic acid sample, characteristic bands were noted at 3544, 3458, 3414, and 3317 cm^{-1}, which correspond to O-H/N-H stretching vibrations. Carbonyl stretching vibration bands occurred at 1684 cm^{-1}, whereas the bands found at 1602, 1569, 1543, 1517, and 1479 cm^{-1} could be attributed to aromatic ring vibrations and amide vibrations (Figure 1B).

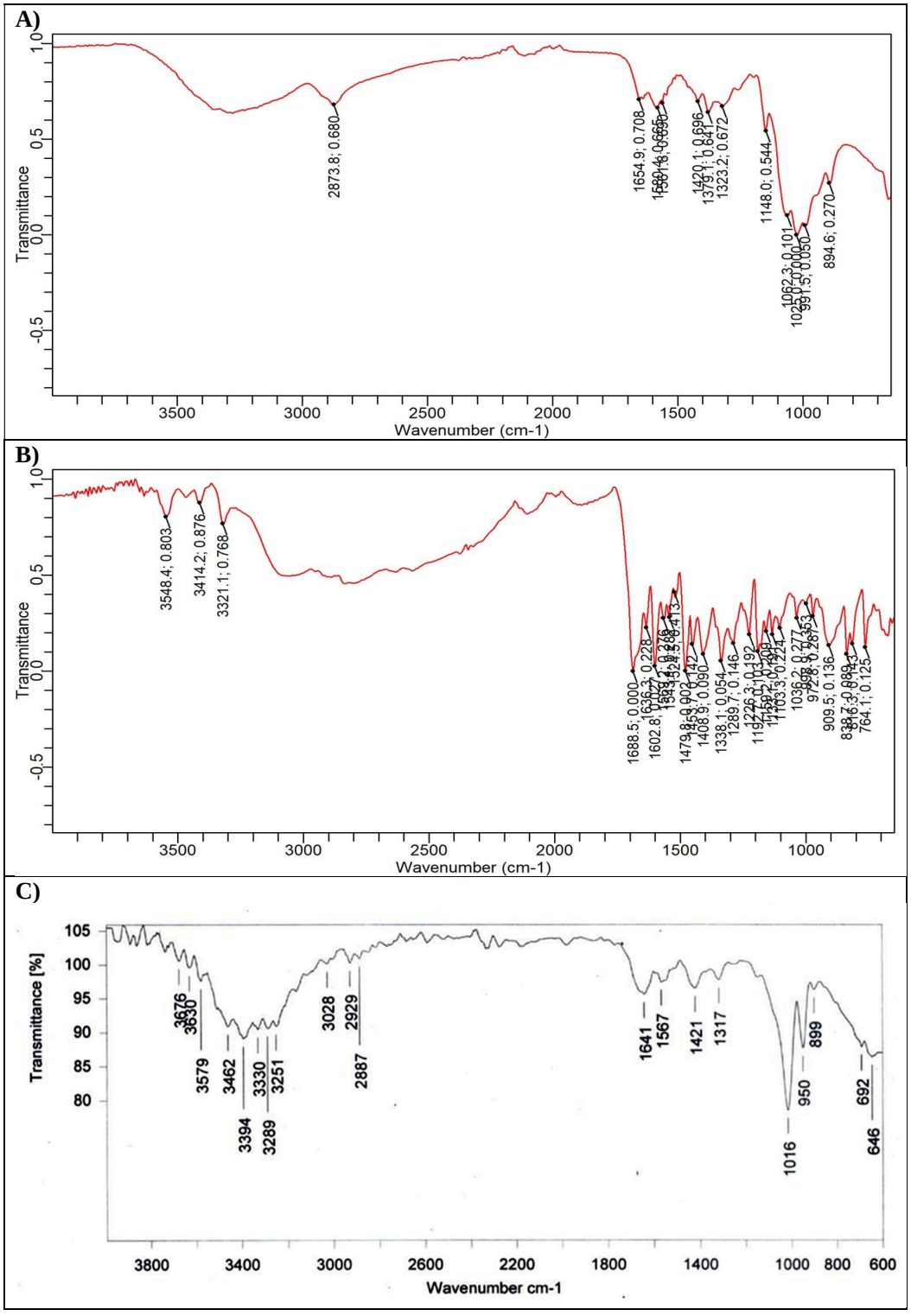

Figure 1. FTIR spectra of (A) chitosan, (B) folic acid, and (C) folic-acid-conjugated chitosan (FA-CS). The important diagnostic wavenumbers are shown to highlight the characteristic functional groups and spectral changes associated with FA-CS conjugation.

The characteristic peaks from the FTIR spectra of FA-CS included a broad region at 3537, 3410, and 3317 cm^{-1}, which corresponded to overlapping O-H/N-H stretching vibrations. In addition, vibration bands observed at 1684 and 1636 cm^{-1} corresponded to carbonyl and amide vibrations, respectively. Amide vibrational bands were found at 1565 and 1543 cm^{-1} (Figure 1C) [47]. It should be noted that several characteristic folic acid peaks were found in the FA-CS sample, such as the band at 1334 cm^{-1} [47].

Overall, FTIR analysis indicated the presence of characteristic functional groups of both chitosan and folic acid in the FA-CS product. However, C-N conjugation or amide bond formation cannot be conclusively verified by FTIR spectroscopy alone. Therefore, the FTIR interpretation was limited to supportive evidence for FA-CS formation, together with the synthesis procedure and purification steps.

3.2. Optimization of 5-fluorouracil-loaded folic acid-conjugated chitosan nanoparticles

3.2.1. Experimental design for optimization of 5-fluorouracil-loaded folic acid-conjugated chitosan nanoparticles by Box–Behnken design

To optimize the formulation of 5-FU-loaded FA–CS nanoparticles, a Box–Behnken design was used. Fourteen experimental runs were carried out as per the design matrix, and the factor settings with the corresponding results are shown in Table 2: Results for Box-Behnken Design for Optimization Batches. Two centre-point batches were included to check the repeatability of the process. The close grouping of these center batches for particle size, PDI, and entrapment efficiency confirmed that the process was consistent and the variation between runs was mainly due to changes in formulation factors rather than random error [48].

Within the experimental range, the FA–CS concentration had the most noticeable effect on particle size increasing polymer levels produced a denser matrix, leading to slightly larger nanoparticles. STPP concentration influenced both particle size and uniformity. STPP at lower levels thus tightened the polymer network and reduced size, while very high concentrations increased viscosity of the dispersion, leading to minor aggregations, resulting in an increased PDI. The amount of 5-FU mainly influenced drug entrapment, with moderate drug loading giving better encapsulation efficiency, while excess drug tended to remain on the surface, lowering %EE [12].

Overall, the results indicated clear relationships among the three formulation factors. The design software fitted the experimental data to a quadratic model that captured the curvature and interaction effects between FA–CS and STPP concentrations. The model diagnostics indicated statistically sound fitting, with high R^2 values and non-significant lack of fit. Multi-response optimization revealed that the best formulation was obtained at moderate levels of polymer, crosslinker, and drug. The optimized batch produced nanoparticles with a particle size of 232.5 nm, PDI of 0.307, and entrapment efficiency of 81.07%, which agreed closely with the predicted results and confirmed the validity of the model.

Table 2. Results for BBD Design for Optimization Batches (OFU1-OFU 14).

Batch Code	Sr. No.	Independent Variables			Dependent Variables		
		FA-CS Concentration	STPP Concentration	Drug Amount	PS (nm)	PDI	% EE
		X1	X2	X3	Y1	Y2	Y3
OFU 1	1	0.3	1	25	687.4	0.559	91.68
OFU 2	2	0.1	0.5	17.5	121.7	0.101	75.26
OFU 3	3	0.3	0.75	17.5	390.5	0.346	85.11
OFU 4	4	0.3	1	10	511.6	0.467	87.12
OFU 5	5	0.5	0.75	25	634.8	0.569	94.55
OFU 6	6	0.3	0.75	17.5	389.5	0.331	84.56
OFU 7	7	0.1	0.75	25	324.7	0.231	77.45
OFU 8	8	0.3	0.5	25	284.9	0.234	77.34
OFU 9	9	0.5	0.75	10	431.5	0.458	87.54
OFU 10	10	0.3	0.5	10	146.4	0.146	79.56
OFU 11	11	0.5	0.5	17.5	321.3	0.312	84.21
OFU 12	12	0.1	1	17.5	421.3	0.289	79.94
OFU 13	13	0.1	0.75	10	216.5	0.129	77.52
OFU 14	14	0.5	1	17.5	756.8	0.698	94.73

CS: Chitosan, STPP: Sodium Tripolyphosphate, FA: Folic Acid: PS: particle size; PDI: polydispersity index; EE: Entrapment efficiency

3.2.2. Statistical analysis for Box-Behnken design

The purpose of the optimization project was to define how specific variables in formulation impacted, predictably, the final attributes of nanoparticles. The use of the Box-Behnken design enabled the development of a mathematical model that can estimate the response for any level of polymer, crosslinker, and drug within the experimental range [48]. Through completing all 14 experiments, in random order, we determined that there was a significant effect for each independent variable on at least one of the response variables measured (particle size (Y_1), PDI (Y_2), and entrapment efficiency (Y_3)[49].

The data from the experiments were analyzed using various statistical models to determine which model best described the relationship between the formulation variables and the formulation responses. The reduced quadratic models were chosen, as opposed to linear, two-factor interaction, and all the quadratic models had sufficient evidence of statistical significance ($p < 0.05$), model fit, and lack-of-fit. The lack-of-fit value was not statistically significant ($p > 0.05$), meaning the predicted responses agreed very well with the experimental responses. These three data sets' key statistical adequacy parameters are listed in Table 3.

The particle size model (Y_1) was a good candidate for nonlinear regression due to a high F-value, a low p-value and good R^2-values among the model fit statistics; hence it can be concluded that the model produced reliable output based on the statistical support provided. For the PDI model (Y_2) there was a close match between the experimental and the predicted responses which supports the conclusion that the developed model could adequately describe the effect of FA-CS, STPP and drug amount on particle size distribution. The model for entrapment efficiency (Y_3) also had acceptable statistical support values with $R^2 = 0.9176$, adjusted $R^2 = 0.809$ and predicted $R^2 = 0.911$; the close match between the adjusted and predicted R^2 statistics provides further evidence of the predictive ability of the models developed in this study within the design space considered. The lack of fit for all three models was non-significant; therefore, the selected reduced quadratic equations adequately described the response behaviour for all three responses and thus provided the foundation for multi-response optimization.

3.2.3. Regression analysis and polynomial equation discussion

The experimental data obtained from the Box–Behnken design were fitted to a quadratic model to understand how each variable influenced the properties of the nanoparticles. The reduced regression equations for particle size (Y_1), polydispersity index (Y_2), and entrapment efficiency (Y_3) are presented below.

$$Y_1=402.78+132.52X_1+187.85X_2+78.23X_3+33.98X_1X_2+23.77X_1X_3$$

$$Y_2=0.3479+0.1609X_1+0.1525X_2+0.0491X_3+0.0495X_1X_2$$

$$Y_3=84.04+6.36X_1+4.64X_2+1.16X_3+1.77X_1X_3+1.7\ X2X3$$

These equations describe how variations in FA–CS concentration (X_1), STPP concentration (X_2), and drug amount (X_3) influence the nanoparticle characteristics. Positive coefficients indicate that an increase in the corresponding variable increases the response, while negative ones would suggest the opposite.

For the particle size (Y_1), the concentration of FA-CS as well as STPP was found to have strong positive effects, which may indicate that the higher the polymer concentration, the larger the particles that are formed, as well as the tendency of the particles to aggregate or associate with each other during the gelation process, possibly due to the increased viscosity of the polymeric solution, leading to the formation of a dense ionic structure during gelation. The influence of the concentration of the polymer as well as the effect of the crosslinking conditions on the particulate characteristics of the chitosan-based colon delivery system has been reported in the previous literature [50, 51].

Table 3. Statistical adequacy parameters of the selected regression models for particle size (Y1), polydispersity index (Y2), and entrapment efficiency (Y3)**.**

Response	Selected model	df	Model F-value	Model p-value	R^2	Adjusted R^2	Predicted R^2	Lack-of-fit p-value	Interpretation
Y1: Particle size (PS)	Reduced quadratic	6	7190.64	< 0.0001	0.9998	1.000*	0.999*	0.7901	Highly significant model with excellent fit and non-significant lack of fit
Y2: Polydispersity index (PDI)	Reduced quadratic	6	306.14	< 0.0001	0.9951	0.991*	0.980*	0.8625	Highly significant model with strong fit and non-significant lack of fit
Y3: Entrapment efficiency (%EE)	Reduced quadratic	5	22.27	< 0.0001	0.9176	0.809*	0.911*	0.7899	Significant model with acceptable fit and non-significant lack of fit

In the case of PDI (Y_2), all the variables had a small positive effect, implying that with an increase in FA-CS, STPP, or drug content, the distribution of the particles' sizes becomes wider. This may imply that too much variation in the formulation level may affect the homogeneity of the nanoparticles. This may result from the fact that too low or too high a ratio of polymers to crosslinkers may interfere with the gelation process, resulting in particles of less homogeneous structure [52]. However, since the optimized formulation showed a PDI within an acceptable range, reasonable homogeneity of the nanoparticles was maintained.

In terms of entrapment efficiency (Y_3), the concentration of FA-CS was found to be the most significant variable, followed by STPP concentration and the interaction between FA-CS and drug (X_1X_3). The increase in polymer concentration may be attributed to the larger volume of the matrix that can entrap more drug through more available functional groups. The appropriate concentration of STPP may contribute to the enhancement of the crosslinked structure by minimizing drug leakage during nanoparticle formation. These variables may contribute to the entrapment efficiency of 5-FU within the chitosan matrix. Previous studies on chitosan-based colon-targeted drug delivery systems showed that matrix density, swelling behavior, and polymer-crosslinker balance may significantly contribute to drug retention/release [51].

Overall, the regression analysis clearly indicated that FA-CS concentration was the most influential factor on all three responses. The fitted equations showed good agreement with the experimental values ($R^2 > 0.99$ for all models), indicating that the model was capable of predicting the responses within the studied design space. These equations therefore served as a useful mathematical tool to guide formulation adjustment and achieve desirable particle size, acceptable uniformity, and improved drug entrapment. The regression coefficients of the fitted full and reduced models are presented in Supplementary table S1, while the corresponding reduced regression equations for Y1, Y2, and Y3 are given below.

Interpretation of response surfaces (Contour and 3D) for Y1, Y2 and Y3

Contour and three-dimensional surface plots gave a clear picture of how formulation components interacted in developing the characteristics of the nanoparticles.

As illustrated in Figure 2 3D Surface Plots, Contour Plots for Responses Y1, Y2 and Y3 and Overlay Plot, for particle size (Y_1), the response surface rose gradually from the lower-left to the upper-right corner of the plot, indicating increased particle size with increased FA-CS and STPP concentrations. The smallest particles were produced when both factors were kept at a low to moderate level. Within this range, the ionic gelation was sufficient to hold the structure but not excessive enough to cause clumping. When FA-CS or STPP exceeded their middle range, particles started to grow larger. This occurred because higher crosslinker and polymer levels increased matrix density and promoted enlargement of the particles during network formation. The plot for PDI (Y_2) was bowl-shaped, having the lowest values concentrated around the center of the design space. This signified that the most homogenous nanoparticles were produced when both FA-CS and STPP were balanced at their intermediate concentrations. Moving toward any extreme (very high or very low levels of the polymer and crosslinker) widened the size distribution. Such an imbalance most likely disturbed the smooth process of gelation, producing particles of heterogeneous sizes and slightly higher PDI values. For entrapment efficiency (Y_3), the surface appeared as a smooth ridge or dome. Entrapment improved steadily as FA-CS concentration increased from low to moderate levels and reached a maximum when STPP was held within its mid-range. Beyond that point, further addition of STPP slightly reduced efficiency. This trend suggested that moderate crosslinking created enough network density to trap the drug efficiently, while excessive crosslinking may have reduced the available internal space for drug accommodation or promoted drug expulsion during particle formation. At very low FA-CS levels, fewer reactive sites were available, resulting in poor drug binding and lower encapsulation (Figure 2).

Overall, the surface plots clearly showed that the best combination for small, uniform, and drug-rich nanoparticles lay in the middle zone of the FA–CS and STPP concentration range. This region formed the optimized design space, where all responses were balanced and the formulation showed consistent, reproducible behaviour.

3.2.4. Checkpoint analysis and formulation optimization

The software executed the model established in order to locate a formulation that would meet all optimization objectives at once which were accomplished using a numerical desirability approach. For example, particle size (Y_1) and (Y_2) were minimized as there is an advantage to having smaller, more uniform nanoparticles in oral nanocarrier systems therefore both should be minimized. Similarly, in order to achieve a higher incorporation of 5-FU into the nanoparticulate matrix, the entrapment efficiency (Y_3) was maximised. Based on these constraints, the software scanned the design space generated by the Box-Behnken design and provided an optimised formulation labelled 0.451 mg/mL FA-CS, 0.504 mg/mL STPP and 10.09 mg (5-FU).

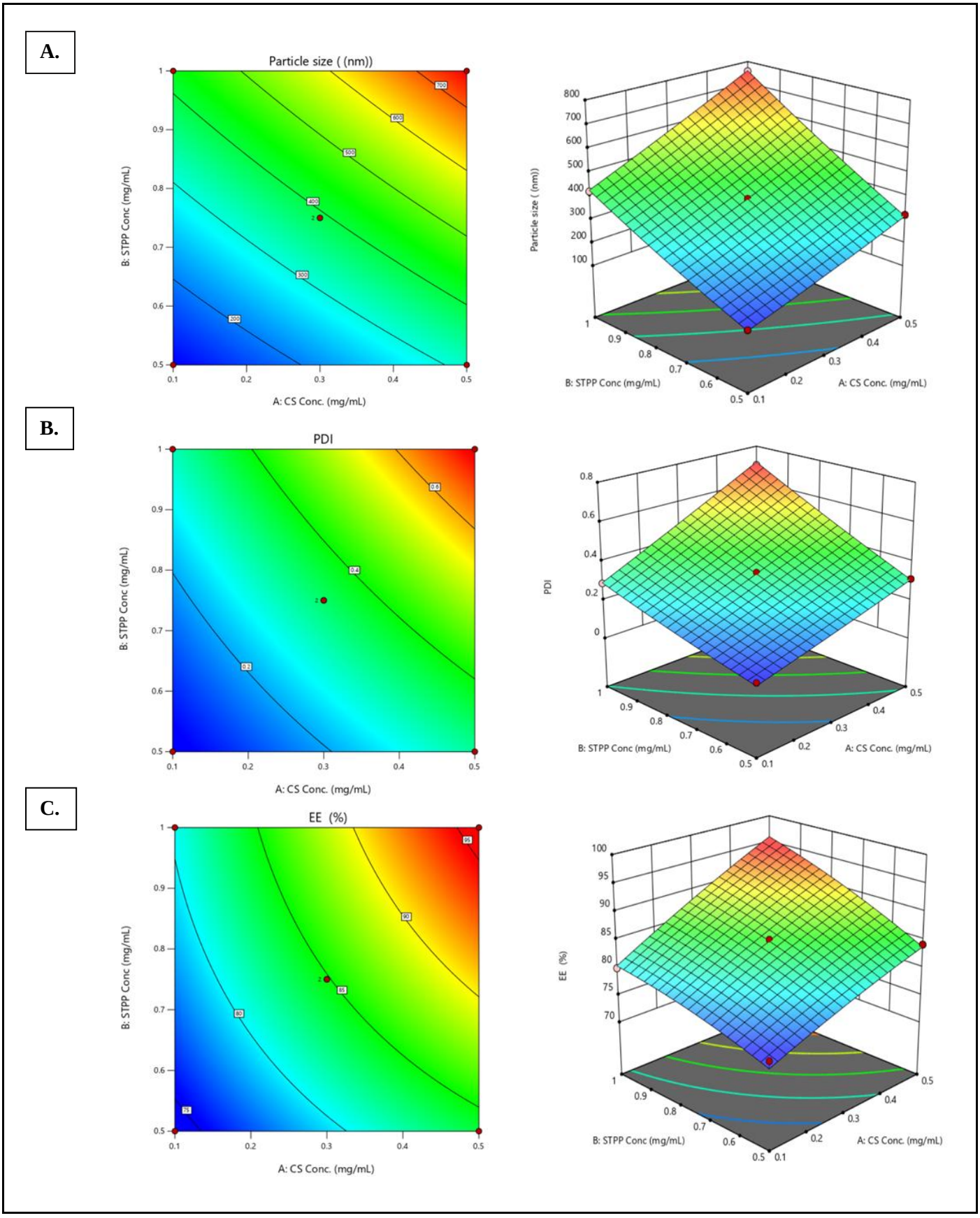

Figure 2. Contour plots and three-dimensional response surface plots showing the effect of folic-acid-conjugated chitosan (FA-CS) concentration and sodium tripolyphosphate (STPP) concentration on (A) particle size, (B) polydispersity index (PDI), and (C) entrapment efficiency (EE) of 5-fluorouracil-loaded FA-CS nanoparticles. (D) Overlay plot showing the optimized design space based on the desired criteria for particle size, PDI, and EE.

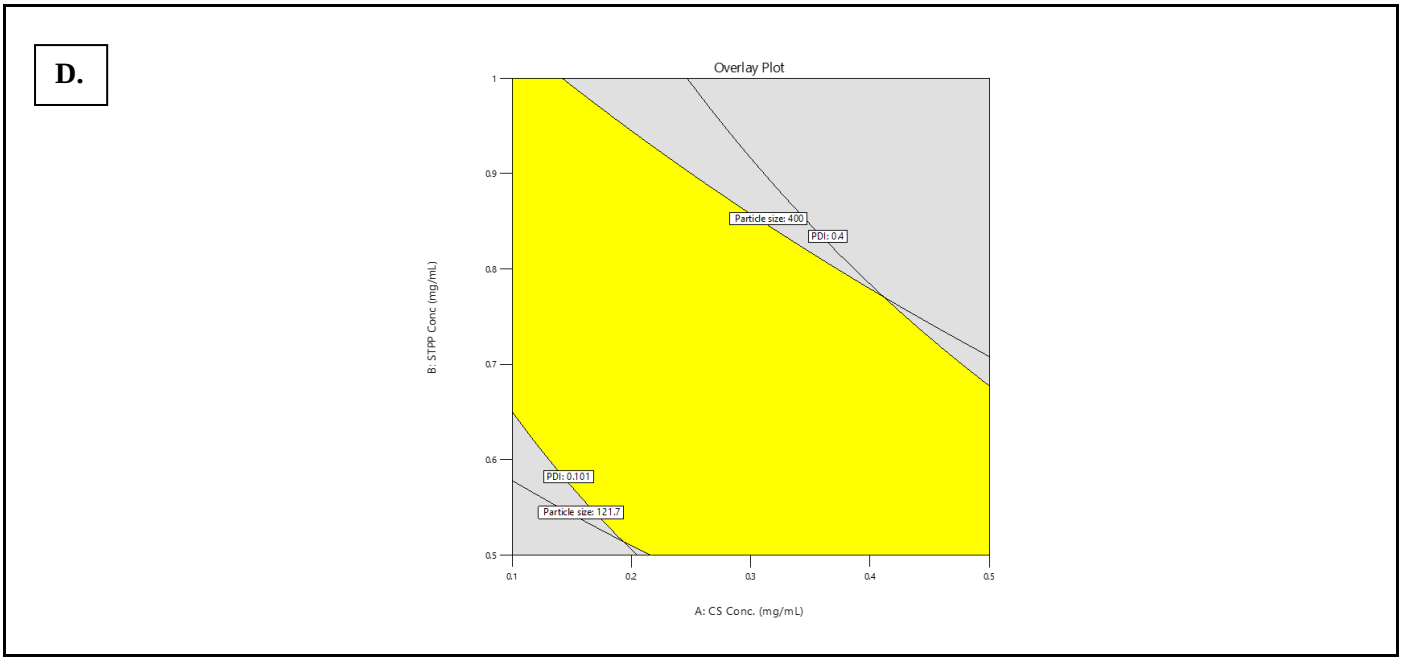

Figure 2. (Continued). Contour plots and three-dimensional response surface plots showing the effect of folic-acid-conjugated chitosan (FA-CS) concentration and sodium tripolyphosphate (STPP) concentration on (A) particle size, (B) polydispersity index (PDI), and (C) entrapment efficiency (EE) of 5-fluorouracil-loaded FA-CS nanoparticles. (D) Overlay plot showing the optimized design space based on the desired criteria for particle size, PDI, and EE.

When this formulation was prepared and tested experimentally, it was found to have a particle size of 238.8 nm, a PDI of 0.319, and an entrapment efficiency of 80.96%, compared to the predicted values of 232.5 nm, 0.307, and 81.07%, respectively. The percentage errors obtained at this checkpoint batch were 2.71% for particle size, 3.91% for PDI, and 0.14% for entrapment efficiency. As all the values are close enough, it was decided that this batch of the formulation (OBEXT 1) was the optimized one, and the method of desirability function was successful.

To validate the robustness and predictive capabilities of the quadratic models, five sets of external checkpoint formulations (OBEXT 1-OBEXT 5) were tested within a feasible region shown in the overlay plot. Values for each particle size, PDI, and entrapment efficiency (along with their corresponding percentage error) are summarized in Supplementary table S2. In general, the experimental responses were consistent with the predicted values of the models. By modifying the predicted errors, particle size ranged from -4.11% to 4.77%, PDI ranged from -0.72% to 8.60%, and entrapment efficiency varied between 0.14%-2.70%. Therefore, it can be concluded that these low predicted error rates support the adequacy of the regression equations and demonstrate that the design space chosen was adequate for formulation optimization.

The overlay plot from the three responses was quite useful. The overlay plot in Figure 2 illustrated the portion of the plot where all three responses were included within acceptable limits. The overlay plot identified one overlapping region where all three responses had the following results: (1) average particle size was <400 nm; (2) PDI was <0.40; and (3) %EE was >75%. This overlapping region is a design space for this nanoparticle system. The design space, from a practical aspect, represents a continuum of FA-CS and STPP concentrations (i.e., drug content near its optimized level) at which the nanoparticles maintain small sizes (i.e., <400 nm), are relatively uniformly sized, and has sufficient loading of 5-FU. Therefore, from a QbD perspective, identification of the design space is important because it characterizes a reasonable range of operating conditions, whereas the optimisation corresponds to one specific condition.

The ability to work within this design space ensures flexibility in formulation development, as changes in the concentration of polymer or crosslinker will not cause the formulation to fall outside the limits. This is particularly important during scale-up and subsequent development, as process variations can sometimes be minor. The Box-Behnken design was useful for understanding the formulation variables and their effects. Since the checkpoint formulations agreed well with the predicted values, the optimized region can be considered practical and reliable.

3.3. Characterization of optimized 5 fluorouracil loaded folic acid conjugated chitosan nanoparticles

3.3.1. Particle size, PDI, and zeta potential analysis

The optimized 5-FU-FA-CS nanoparticles showed an average particle size of about 232.5 nm with

A.

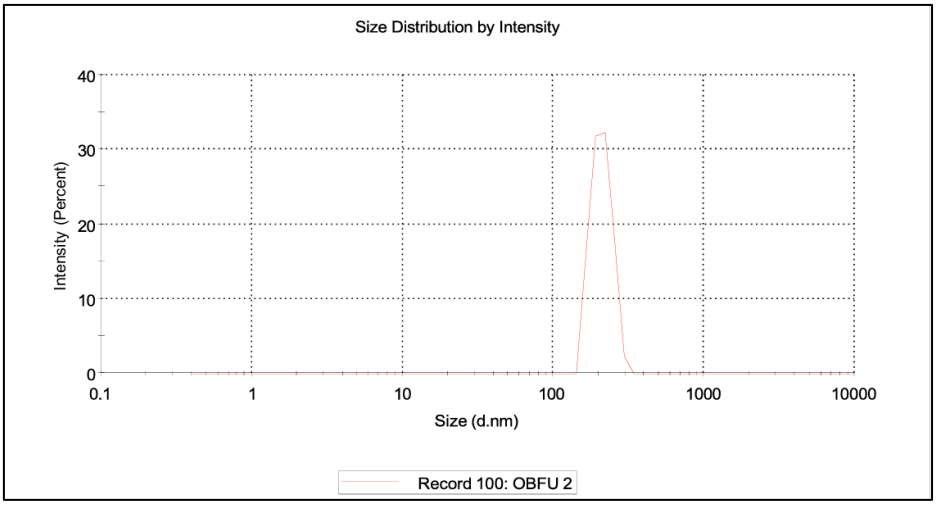

B.

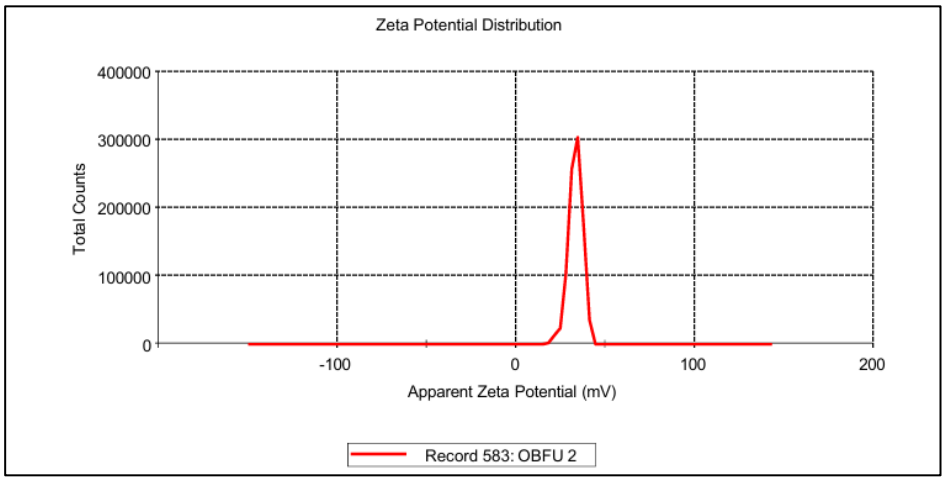

C.

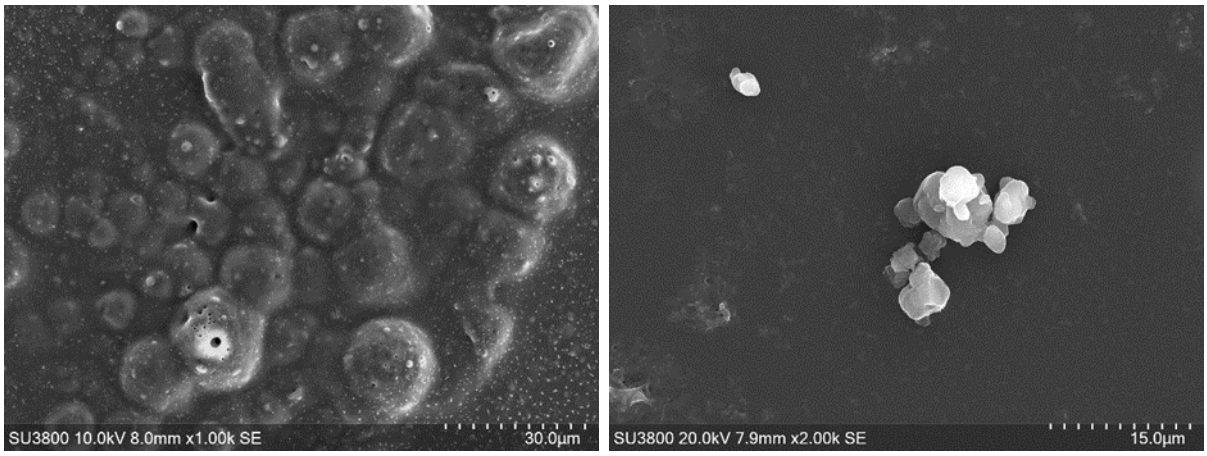

Figure 3. (A) Particle size distribution of optimized 5-fluorouracil-loaded folic acid-conjugated chitosan nanoparticles (5-FU-FA-CS nanoparticles), (B) zeta potential (mV), (C) scanning electron microscopy (SEM) image of the optimized batch, and (D) particle size distribution of re-dispersed 5-FU-FA-CS nanoparticles recovered from compressed tablets.

D.

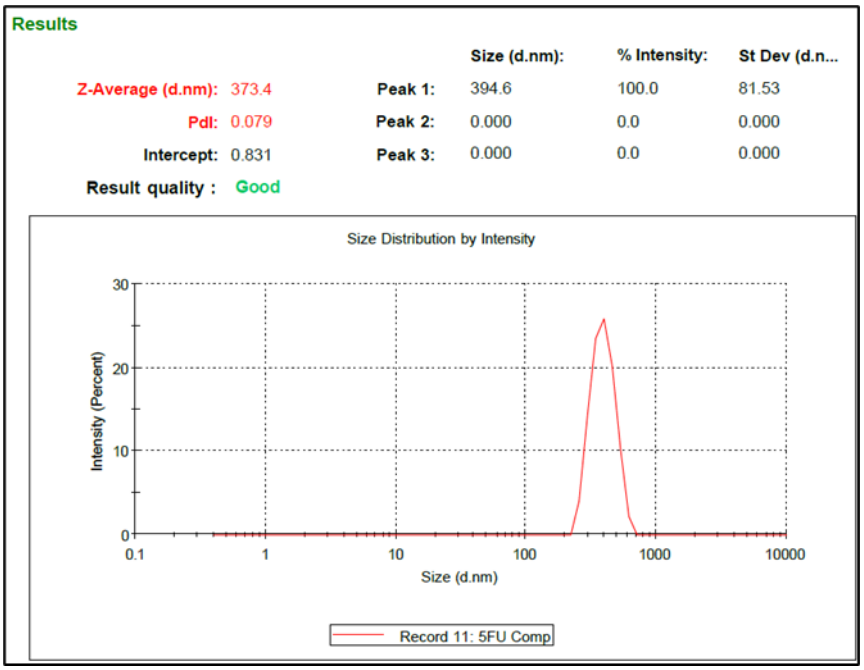

Figure 3. (Continued). (A) Particle size distribution of optimized 5-fluorouracil-loaded folic acid-conjugated chitosan nanoparticles (5-FU-FA-CS nanoparticles), (B) zeta potential (mV), (C) scanning electron microscopy (SEM) image of the optimized batch, and (D) particle size distribution of re-dispersed 5-FU-FA-CS nanoparticles recovered from compressed tablets.

a PDI of 0.307**,** indicating a reasonably uniform size distribution (Figure 3A). The zeta potential was +24.1 mV, indicating a sufficiently positive surface charge that may contribute to electrostatic stabilization and reduced aggregation tendency (Figure 3B). These results confirmed that the formulation produced stable, well-dispersed nanoparticles suitable for colon-targeted delivery. Nanoscale particle size is also considered favorable for improving surface interaction with the biological environment and supporting efficient drug carrier performance**.**

3.3.2. Morphological characterization by SEM

The optimized 5-FU-FA-CS nanoparticles were analyzed under a scanning electron microscope (SEM) to have an idea of their surface appearance. The particles have a round and smooth appearance. The large clusters of particles observed in the SEM image may have been caused by the aggregation of the nanoparticles during the drying and preparation of the particles for the SEM (as seen in Figure 3C). Therefore, the SEM was used to determine the shape of the particles and their surface texture. The size of the particles was better estimated using DLS, which gave a mean diameter of 232.5 nm. The shape of the particles obtained from the SEM image confirms that the nanoparticle system was formed.

3.3.3. % Yield

The percentage yield of the three best batches of nanoparticles from DoE was determined by calculating the particle and theoretical yield, and the results were 93.92 ± 0.672 %.

3.3.4. Entrapment efficiency (%EE)

The drug entrapment efficiency of the optimized 5-FU-FA–CS nanoparticles was found to be around 81.3%, showing that most of the drug was successfully incorporated within the polymeric matrix. The high entrapment can be attributed to the strong interaction between 5-FU and the amino groups of chitosan, as well as the stable crosslinking formed by STPP.

3.3.5. % Drug Content

The drug content of the optimized batch of the nanoparticles was calculated and were observed to be 88.12 ± 0.07%.

3.3.6. In vitro Drug Release Studies

The release of 5-FU from the optimized nanoparticles was evaluated at two different pH conditions

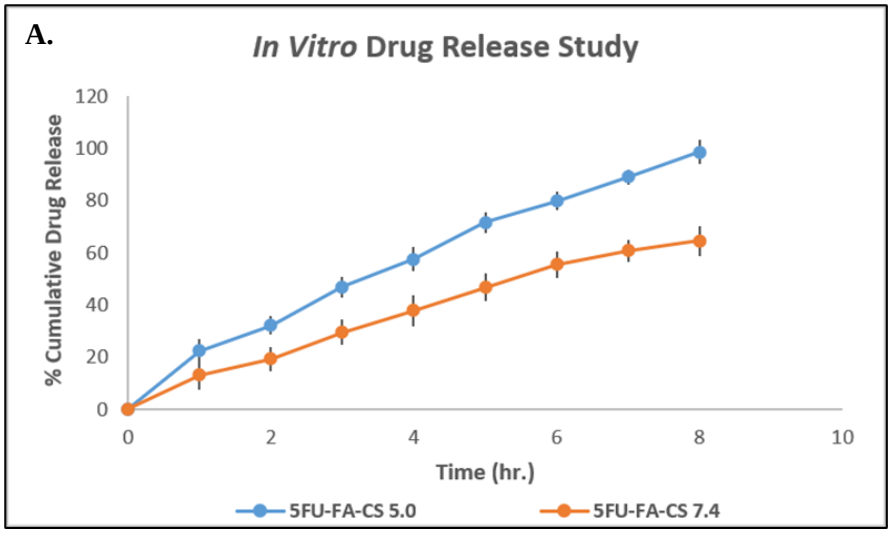

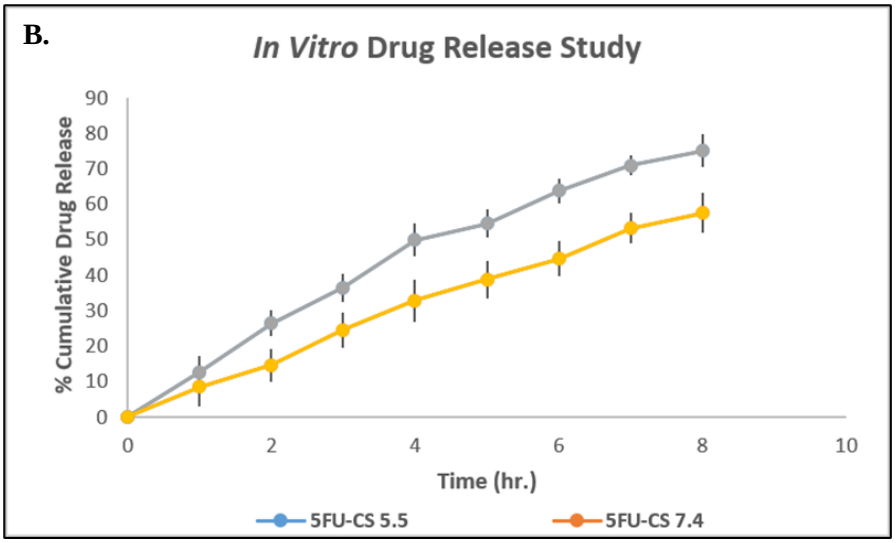

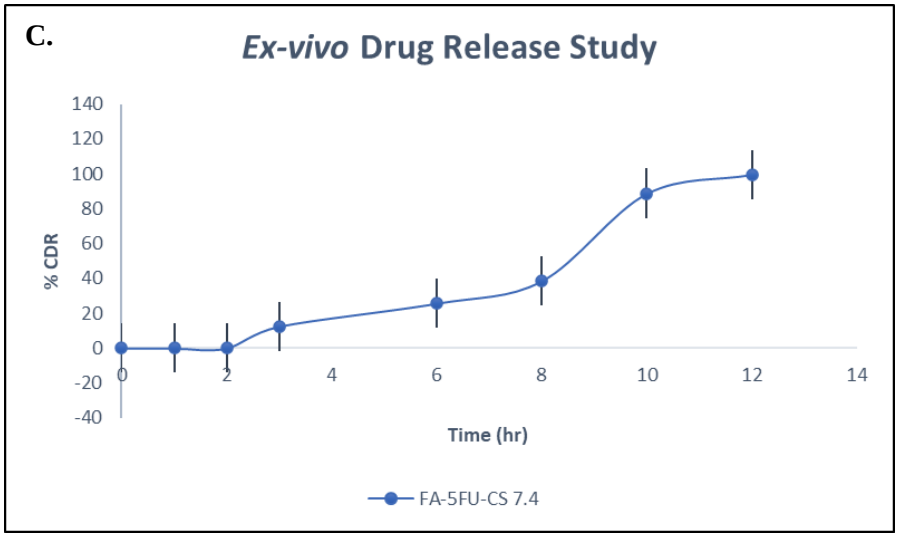

Figure 4. *In vitro* cumulative drug release profiles of (A) optimized 5-fluorouracil-loaded folic acid-conjugated chitosan nanoparticles (5-FU-FA-CS nanoparticles) at pH 5.0 and pH 7.4, and (B) 5-fluorouracil-loaded unconjugated chitosan nanoparticles (5-FU-CS nanoparticles) at pH 5.5 and pH 7.4. (C) *Ex vivo* colonic release/permeation profile of optimized 5-FU-FA-CS nanoparticles using the non-everted rat colonic sac model. Data are expressed as mean ± standard deviation (SD), $n = 3$.

to simulate the physiological (pH 7.4) and tumor/colonic microenvironment as shown in Figure 4. A gradual and sustained release profile was observed in both media, but the rate of drug release was clearly higher at pH 5.0 compared to pH 7.4. At pH 5.0, the 5-FU-loaded FA-CS nanoparticles showed a cumulative drug release of about 98.5% after 8 hours (Figure 4A), while at pH 7.4, the release reached only about 64.5% over the same period (Figure 4B). This difference can be explained by the partial protonation of chitosan in the acidic environment, which likely increased polymer swelling and matrix relaxation, thereby facilitating faster diffusion of the drug. In contrast, at neutral pH, the polymer network remained more compact, resulting in slower release.

The overall pattern confirmed the pH-responsive behavior of the FA-CS nanoparticles, which is desirable for colon-targeted and tumor-site-specific delivery of 5-FU. The slower release at pH 7.4 minimizes premature drug loss in the upper gastrointestinal tract, while the faster release at acidic pH supports efficient drug availability at the cancer site. This biphasic behaviour indicates that the nanoparticle system was able to retain a substantial fraction of the drug under less favorable release conditions while still allowing rapid liberation in an acidic environment, which may be beneficial for improving local drug availability at the target site.

Several kinetic models, including zero-order, first-order, Higuchi, and Korsmeyer-Peppas, as well as Hixson-Crowell, were employed to analyze the *in-vitro* release pattern of the final formulation containing 5-FU-FA-CS nanoparticles. The corresponding R^2 values for all tested models, together with the release exponent (n) from the Korsmeyer-Peppas model, are presented in Table 4. Among these models, the release data showed the highest degree of linearity with the Korsmeyer-Peppas model (R^2 = 0.9970), followed closely by the Hixson-Crowell model (R^2 = 0.991), whereas the R^2 values for the zero-order, first-order, and Higuchi models were 0.955, 0.981, and 0.9496, respectively. This suggests that drug release was governed mainly by diffusion from the polymeric matrix along with matrix relaxation effects. In the Korsmeyer-Peppas model, the value of "n" was found to be below 1, indicating a non-Fickian release mechanism. This suggests that the release occurred through a combination of diffusion and polymer erosion/swelling mechanisms within the matrix, as observed in the optimized 5-FU-FA-CS nanoparticles batch. This behavior is consistent with the pH-responsive chitosan-based nanoparticulate system, where both drug diffusion and structural changes in the polymer network contribute to overall release.

3.3.7. Ex vivo colonic release/permeation study of optimized 5-FU-FA-CS nanoparticles

We utilized a non-everted rat colonic sac model to evaluate the *ex vivo* colonic release/permeation behaviour of optimized 5-FU-FA-CS nanoparticles following an *ex vivo* delivery system via the colon. As presented in Figure 4C, cumulative 5-FU detected in the external medium exhibited a gradual increase over 12 h. The initial two hours demonstrated little to no 5-FU release/permeation through the colonic mucosa; however, from 2 to 8 h, a gradual increase was observed, after which there was a substantial increase at the tenth hour of approximately 95.97 % at 10 hours, with near-complete 5-FU release/permeation after 12 hours.

The observed pattern indicates that the nanoparticle system could maintain a slower initial release/permeation phase and subsequently exhibit increased transfer of 5-FU across the colonic tissue with time. The lower release/permeation observed at early time points may be attributed to the time required for hydration and relaxation of the FA-CS matrix, whereas the later increase may reflect progressive matrix loosening and continued diffusion of the drug through the colonic membrane. Overall, the *ex vivo* results indicate that optimized 5-FU-FA-CS nanoparticles are capable of producing sustained drug availability within the colon and provide additional biologically relevant support beyond *in vitro* release testing.

3.4. Evaluation of core tablets containing 5-fluorouracil-loaded folic acid-conjugated chitosan nanoparticles

As illustrated in Table 5 all three batches of 5-FU-FA-CS nanoparticles loaded core tablets (F1-F3) showed uniform thickness, acceptable hardness, and very low friability (<1%), indicating good mechanical strength. The drug content was consistent across all batches, confirming uniform distribution of nanoparticles within the tablets and suitability for coating. These findings indicate that the compression process produced mechanically robust core tablets without adversely affecting content uniformity. The satisfactory pre-coating properties were important to ensure that the tablets could withstand subsequent coating steps without cracking or excessive weight variation.

Table 4. Kinetic model fitting parameters for in-vitro release of optimized 5-FU-FA-CS nanoparticles at pH 5.0.

Batch	Zero-order (R^2)	First-order (R^2)	Higuchi (R^2)	Korsmeyer-Peppas (R^2)	n	Hixson-Crowell (R^2)
5-FU-FA-CS-NPs	0.934	0.974	0.9294	0.9970	0.737	0.991

Table 5. Evaluation of core tablets containing 5-FU-FA–CS nanoparticles.

Parameters	F1	F2	F3
Thickness (mm)	3.23 ± 0.012	3.33 ± 0.015	3.39 ± 0.016
Diameter (mm)	9.03 ± 0.002	9.01 ± 0.007	9.04 ± 0.003
Hardness (kg/cm²)	4.9 ± 0.124	5.0 ± 0.216	5.1 ± 0.163
Friability (%)	0.36	0.42	0.37
Weight uniformity (mg) *	256.1 ± 0.83	253.5 ± 0.98	246.9 ± 0.49
Drug content (%) #	92.25	94.96	96.35
Value shown as mean ± SD where, n=3, *n=20, #n=10			

3.4.1. Re-dispersion study of nanoparticles after tablet compression

In order to assess if the integrity of the nanoparticles had been compromised as a result of the direct compression method of preparation, re-dispersion analysis of the optimized 5-FU-FA-CS nanoparticles loaded core tablets was carried out. The re-dispersed particles were analyzed to determine their particle size and PDI and compared to those of the optimized nanoparticles before compression.

The optimized nanoparticles before compression had a particle size of 232.5 nm and a PDI of 0.307. The re-dispersed particles had a Z-average particle size of 373.4 nm and a PDI of 0.079 (Figure 3D). The results show that the direct compression method of preparation had an influence on the particle size of the nanoparticles. The particles were in the colloidal submicron range and had a narrow particle size distribution. The low PDI of the re-dispersed particles shows that the particulate system remained relatively uniform and did not aggregate to any great extent.

From the re-dispersion analysis of the nanoparticle-loaded tablets prepared by the direct compression method of preparation, it is clear that the 5-FU-FA-CS nanoparticles loaded tablets can release the nanoparticle system after compression. The increase in particle size of the re-dispersed particles is insignificant and shows that the direct compression method of preparation is suitable for the development of the colon-targeted formulation.

3.5. Coating of core tablets

The colon-targeted tablets, therefore, consisted of a core coated with multiple coats of three different polymers arranged in a defined sequence to ensure site-specific drug release. Three coats of Eudragit E100 were applied adjacent to the core as the inner release-modulating layer, followed by one coat of HPMC K15M as the intermediate separating barrier, and two coats of Eudragit S100 as the outer pH-dependent protective layer. The applied coating was carried out using the dip-coating method with subsequent drying at 40 ± 0.5 °C. The gradual increase in tablet weight after each coating confirmed successful deposition of the polymer layers and suggested reasonably uniform coating over the tablet surface, as shown in Supplementary table S3. This sequential coating approach was intended to minimize premature drug release in the upper gastrointestinal tract and promote release at the colonic pH, in line with the design objective of the formulation. The percentage weight gain during coating was recalculated and is now presented as cumulative increase relative to the initial core tablet weight.

3.5.1. Coating integrity testing

Coating integrity testing was carried out on dummy tablets (average weight 250 mg) to determine the number of coating layers required for Eudragit E100 and Eudragit S100 before finalizing the multilayer coating design**.** The strength of the coated tablets and their ability to remain intact were tested under conditions that simulated both stomach and intestinal environments. The results indicated that the outer Eudragit S100 coating was sufficient to protect the tablets in 0.1 N HCl (pH 1.2), preventing premature disintegration under gastric conditions. In contrast, the inner Eudragit E100 coating helped maintain tablet integrity in PBS (pH 7.4), thereby delaying release in the intestinal phase. The integrity test was performed separately for individual Eudragit E100 and Eudragit S100 coats and was not conducted after application of each layer of the final multilayer-coated tablet. HPMC K15M was not subjected to separate integrity optimization, as it was incorporated as a fixed intermediate barrier layer between the Eudragit E100 and Eudragit S100 coats. Hence, it can be concluded that two coats of Eudragit S100 were adequate for gastric protection, while three coats of Eudragit E100 contributed to maintaining tablet integrity during the subsequent intestinal stage (Supplementary table S4). Based on these observations, the final multilayer coating architecture was selected as three coats of Eudragit E100, one coat of HPMC K15M, and two coats of Eudragit S100 over the core tablet. Therefore, these preliminary findings were used to select the coating levels for the final multilayer tablet system, which was

intended to protect the core until it reached the colon, where drug release was triggered. These findings support the functional role of the sequential coating system in restricting premature release and improving site-specific delivery of 5-FU to the colon.

3.5.2. Post-coating quality control analysis of tablets

The general appearance and physical properties of all coated tablets were checked after coating. All the coated tablets possessed smooth, even surfaces without any cracks, peeling, or color variation; this reflects good control of the coating process. The average thickness and weight showed a slight increase after coating, due to the addition of successive polymer layers. Hardness and friability also remained within acceptable limits, showing that the coating did not adversely affect the mechanical strength of the tablets. Drug content analysis confirmed that 5-FU was uniformly distributed across all coated tablets with minimal variation among batches. These results indicate that the coating process was reproducible and did not compromise the physical integrity or content uniformity of the final tablets. Such post-coating quality is important to ensure consistent performance during subsequent release testing.

Overall, the post-coating evaluation confirmed that the resultant tablets had complied with the required quality standards for appearance, mechanical strength, and drug content, warranting them for further *in vitro* testing.

3.5.3. In vitro drug release studies

The drug release study indicated that, at 0.1 N HCl (pH 1.2), there was no drug release from the coated tablet batches (F1-F3), confirming that the Eudragit S100 layer appropriately protected the core tablets in the acidic stomach. This can be explained by the nature of Eudragit S100, which remains insoluble at low pH but starts dissolving and permitting drug release only at higher pH. Moving into phosphate buffer pH 7.4, after an initial lag, a small gradual release was observed, showing about 12-29% drug release, indicating the onset of medium penetration through the coating system. The HPMC K15M middle layer slowly absorbed the medium and formed a gel barrier that contributed to retarding premature release. A minor increase in drug diffusion was noticed due to the softening of Eudragit E100 around pH 5, where it became slightly permeable. At around pH 7.0, E100 dissolved and the medium slowly penetrated into the core and favored continuous release of the drug. During the later stage, the entry of the formulation into the colon-like environment enhanced the drug release due to polymer swelling, matrix relaxation, and partial depolymerization of chitosan by colonic enzymes. Similar swelling-triggered release behavior of chitosan-based compression-coated systems has also been reported previously [53]. The final cumulative drug release within 12 hours ranged between 92 to 96%, and batch F3 showed the maximum release, 96.41 ± 0.30%, possibly due to its higher proportion of microcrystalline cellulose, which facilitated the entry and diffusion of water (Figure 5).

Overall, the triple-layer coating of Eudragit E100, HPMC K15M, and Eudragit S100 effectively prevented early drug leakage in the stomach and intestine while ensuring a controlled and targeted release in the colon. The observed release sequence supports the functional role of the multilayer system,

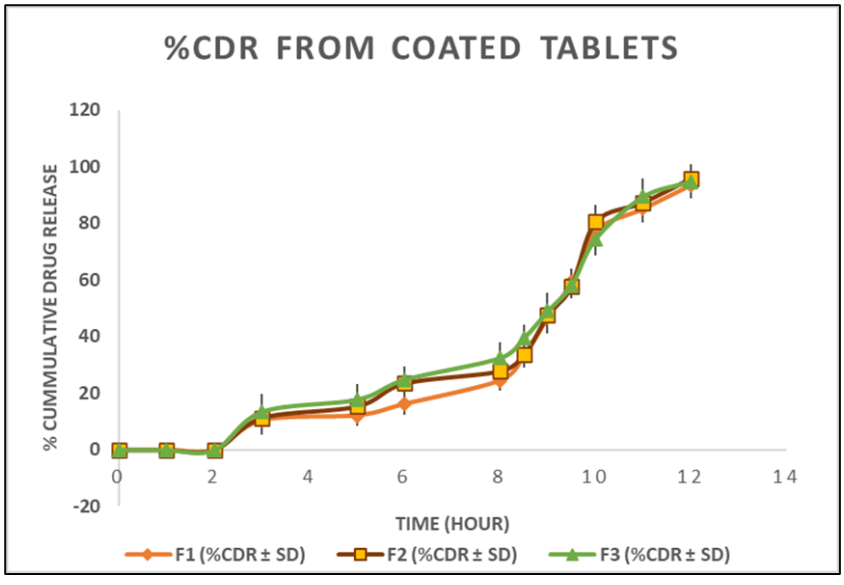

Figure 5. *In vitro* cumulative drug release profiles of coated 5-FU-FA–CS nanoparticle tablets (F1–F3) showing sustained and controlled release behavior over 12 h. Data are expressed as mean ± SD, n = 3.

Table 6. Kinetic model fitting parameters for *in vitro* release of coated 5-FU-FA-CS nanoparticle tablets.

Formulation	Zero-order R^2	First-order R^2	Higuchi R^2	Korsmeyer-Peppas R^2	n value	Hixson-Crowell R^2
F1	0.8538	0.8712	0.9021	0.9621	0.526	0.9461
F2	0.8798	0.9125	0.9256	0.9787	0.587	0.9256
F3	0.9551	0.981	0.9496	0.9920	0.645	0.9456

where gastric protection, delayed intestinal penetration, and enhanced colonic release were achieved in a stepwise manner. This behaviour is consistent with the intended design of the formulation for colon-targeted delivery of 5-FU.

3.5.4. Drug release kinetics studies

Coated tablet formulations (F 1-F 3) were characterized based on their drug release patterns using several different models to evaluate the mechanism of drug release/kinetics of each formula (zero order, first order, Higuchi, Korsmeyer-Peppas, Hixson-Crowell). The observed overall kinetic parameters for each of the coated tablet formulations are reported in Table 6. The Korsmeyer-Peppas model provided the best fit for the data collected from all three formulations (F1, R^2 = 0.9621; F2, R^2 = 0.9787; F3, R^2 = 0.9920), indicating that combined mechanisms (diffusion and polymer relaxation) were involved in the release of the drug from the coated tablets via an anomalous (non-Fickian) transport mechanism.

3.5.5. Stability study

The stability of optimized 5-FU-FA–CS colon-targeted tablets was studied in accordance with the ICH Q1A(R2) guidelines. For this, all the tablets were enclosed in aluminum foil laminated with polyethylene to safeguard them from light and moisture. Samples were stored under accelerated conditions of 40 ± 2 °C / 75 ± 5 % RH for three months, with periodic evaluation of any changes in appearance and also of drug content and drug release.

During the three-month study, the tablets maintained their original shape and glossy appearance, with no cracking or discoloration observed. The drug content showed only a slight reduction from 96.45 % to 94.32 %, which remained well within acceptable limits. The similarity factor (F_2 = 76.53) reflects that the dissolution profile of the stored tablets was almost identical to that of the fresh batch (Table 7) (Figure 6). In general, the formulation remained physically stable and chemically consistent under the conditions of accelerated studies. These results indicate that the coated tablets possess good stability and maintain their performance during storage. Long-term studies at 25 ± 2 °C / 60 ± 5 % RH are being continued to confirm the final shelf-life.

4. CONCLUSION

The present study successfully formulated and optimized dual-triggered colon-targeted 5-FU tablets incorporating FA-CS nanoparticles using a QbD and Box–Behnken design approach. The optimized formulation demonstrated nanosized, uniform, and stable particles with high drug entrapment efficiency and desirable pH-responsive release behavior. The coated tablets effectively restricted premature drug release in gastric and intestinal environments while ensuring complete and sustained delivery in simulated colonic conditions, confirming their suitability for site-specific CRC therapy. Stability studies under accelerated conditions further verified the formulation's physical and chemical integrity, indicating promising shelf-life potential. Overall, this study highlights a rational and systematic design strategy for developing nanocarrier-based colon-targeted systems capable of improving 5-FU bioavailability and minimizing systemic toxicity. Future *in vivo* and pharmacokinetic evaluations are warranted to establish clinical translation potential and therapeutic superiority of this QbD-driven nanocarrier system for CRC management.

5. ACKNOWLEDGEMENTS

Authors would like to express their gratitude to Dr. Ketan V. Shah and Shree Naranjibhai Lalbhai Patel College of Pharmacy, Umrakh – 394345, Gujarat, India for providing all necessary research facility.

Table 7. Stability evaluation of optimized coated tablets.

Parameters	Initial	After 3 months (40 ± 2 °C / 75 ± 5 % RH)
Appearance	White, round tablets with glossy surface	No visible change; smooth glossy surface retained
Drug content (%)	96.45	94.32
Similarity factor (F_2)	-	76.53

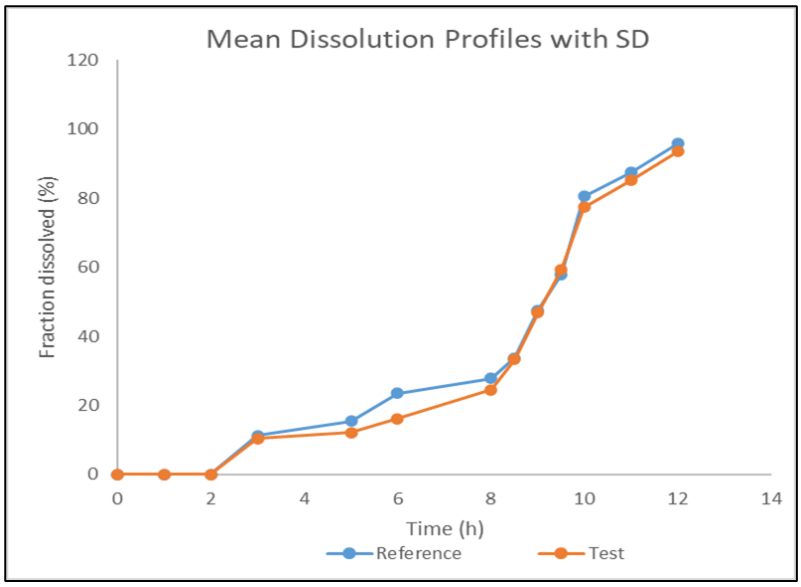

Figure 6. Similarity factor evaluation.

Author contribution

Yash D Dudhwala: Conceptualization & Wrote the manuscript. Riya K. Mehta: Wrote the manuscript, Methodology. Vinod D. Ramani: Wrote the manuscript, Software. Dhiren P. Shah: Reviewed the manuscript. Devesh U Kapoor: Reviewed the manuscript and Project administration.

Funding

None to declare

Conflict of interest

The authors declare that they have no known competing financial interests or personal relationships that could have appeared to influence the work reported in this paper.

Ethics approval

The *ex vivo* study using rat colonic tissue was approved by the Institutional Animal Ethics Committee of Shree Naranjibhai Lalbhai Patel College of Pharmacy, India (approval no. CCDES/SNLPCP/IAEC/26/01/190).

Article info*:*

Received January 3, 2026
Received in revise form May 22, 2026
Accepted June 19, 2026

Data availability

Supplement information is provided upon request**.**

REFERENCES

1. Tsokkou S, Konstantinidis I, Papakonstantinou M, Chatzikomnitsa P, Liampou E, Toutziari E, et al. Sex differences in colorectal cancer: epidemiology, risk factors, and clinical outcomes. J Clin Med. 2025;14(15):5539.
2. Stephens KR, Donica WR, Egger ME, Philips P, Scoggins CR, McMasters KM, et al. Observed changes in the distribution of colon cancer metastasis: A National Cancer Database review and institutional experience. Ann Surg Oncol. 2025;32(1):418-23.
3. Yang Z, Cespedes-Acuña CL, Yang Z, Abu Bakar MZ, Chan KW, Deng X. Plant foods and their bioactives as dietary enhancers for colon cancer treatment with 5-fluorouracil. Food Rev Int. 2025;41(5):1390-439.
4. Hui B, Zhou C, Xu Y, Wang R, Dong Y, Zhou Y, et al. Exosomes secreted by Fusobacterium nucleatum-infected colon cancer cells transmit resistance to oxaliplatin and 5-FU by delivering hsa_circ_0004085. J Nanobiotechnology. 2024;22(1):62.
5. Hanan H, Pervaiz F, Ijaz M, Javaid SM, Bukhari AN, Arshad T, et al. Revolutionizing colon cancer therapy by site-specific 5-fluorouracil delivery with novel stimuli-responsive mucoadhesive hydrogel: optimization via response surface methodology. J Drug Deliv Sci Technol. 2024;92:105358.
6. Manzanares-Guevara LA, Gasperin-Bulbarela J, Cabanillas-Bernal O, Renteria-Maciel M, Licea-Claverie A, Méndez ER, et al. Preparation of pH-sensitive nanogels bioconjugated with shark antibodies (VNAR) for targeted drug delivery with potential applications in colon cancer therapies. PLoS One. 2024;19(1):e0294874.
7. Zhao S, Wang T, Shi K, Li T, Zhu Q, Li Y, et al. 5-Fluorouracil-methotrexate conjugate enhances the efficacy of 5-fluorouracil in colorectal cancer therapy. Invest New Drugs. 2025;43(1):30-41.
8. Ma Y, Thurecht KJ, Coombes AG. Development of enteric-coated, biphasic chitosan/HPMC microcapsules for colon-targeted delivery of anticancer drug-loaded nanoparticles. Int J Pharm. 2021;607:121026.
9. Ding H, Tan P, Fu S, Tian X, Zhang H, Ma X, et al. Preparation and application of pH-responsive drug delivery systems. J Control Release. 2022;348:206-38.
10. Wagner J, Gößl D, Ustyanovska N, Xiong M, Hauser D, Zhuzhgova O, et al. Mesoporous silica nanoparticles as pH-responsive carrier for the immune-activating drug resiquimod enhance the local immune response in mice. ACS Nano. 2021;15(3):4450-66.
11. Sathiyaseelan A, Saravanakumar K, Manivasagan P, Jeong MS, Jang E-S, Wang M-H. Folic acid conjugated chitosan encapsulated palladium nanoclusters for NIR triggered

photothermal breast cancer treatment. Carbohydr Polym. 2022;280:119021.
12. Abbasi M, Sohail M, Minhas MU, Mahmood A, Shah SA, Munir A, et al. Folic acid-decorated alginate nanoparticles loaded hydrogel for the oral delivery of diferourylmethane in colorectal cancer. Int J Biol Macromol. 2023;233:123585.
13. Al-Nemrawi NK, Altawabeyeh RM, Darweesh RS. Preparation and characterization of docetaxel-PLGA nanoparticles coated with folic acid-chitosan conjugate for cancer treatment. J Pharm Sci. 2022;111(2):485-94.
14. Talebian S, Schofield T, Valtchev P, Schindeler A, Kavanagh JM, Adil Q, et al. Biopolymer-based multilayer microparticles for probiotic delivery to colon. Adv Healthc Mater. 2022;11(11):2102487.
15. Han M, Shen N, Tan W, Wang X, Liu Y, Liang J, et al. Layer-by-layer coated probiotics with chitosan and liposomes exhibit enhanced therapeutic effects for DSS-induced colitis in mice. Int J Biol Macromol. 2024;269:132063.
16. Bhaskaran NA, Jitta SR, Kumar L, Sharma P, Kulkarni OP, Hari G, et al. Folic acid-chitosan functionalized polymeric nanocarriers to treat colon cancer. Int J Biol Macromol. 2023;253:127142.
17. Ghosh T, Mandal M, Shee M, Das TK, Mandal M, Banerji P, et al. Fabrication of folic acid-derived carbon dot-conjugated chitosan nanospheres as theragnostic agents for pH-responsive anticancer drug delivery. ACS Appl Bio Mater. 2025;8(4):3096-110.
18. Kesharwani P, Halwai K, Jha SK, Al Mughram MH, Almujri SS, Almalki WH, et al. Folate-engineered chitosan nanoparticles: next-generation anticancer nanocarriers. Mol Cancer. 2024;23(1):244.
19. Algharib SA, Dawood A, Zhou K, Chen D, Li C, Meng K, et al. Preparation of chitosan nanoparticles by ionotropic gelation technique: Effects of formulation parameters and *in vitro* characterization. J Mol Struct. 2022;1252:132129.
20. Ding Z, Chen W, Jiang F, Mo M, Bi Y, Kong F. Synthesis, characterization and *in vitro* digestion of folate conjugated chitosan-loaded proanthocyanidins nanoparticles. Food Res Int. 2023;163:112141.
21. Panigrahi D, Sahu PK, Swain S, Verma RK. Quality by design prospects of pharmaceuticals application of double emulsion method for PLGA loaded nanoparticles. SN Appl Sci. 2021;3:1-21.
22. Hidayat AF, Wardhana YW, Suwendar S, Mohammed AFA, Mahmoud SA, Elamin KM, et al. A review on QbD-driven optimization of lipid nanoparticles for oral drug delivery: from framework to formulation. Int J Nanomedicine. 2025;20:8611-51.
23. Ain QU, Zeeshan M, Mazhar D, Zeb A, Afzal I, Ullah H, et al. QbD-based fabrication of biomimetic hydroxyapatite embedded gelatin nanoparticles for localized drug delivery against deteriorated arthritic joint architecture. Macromol Biosci. 2024;24(2):2300336.
24. Dudhwala YD, Kapoor DU, Mehta RK, Shah DP, Ramani VD, Dedania RR, et al. Strategic formulation and optimization of a febuxostat nanoparticles infused topical gel using Quality-by-Design principles for enhanced therapeutic efficacy in gout management. ChemistrySelect. 2025;10(34):e00972.
25. Mandpe S, Kole E, Parate V, Chatterjee A, Mujumdar A, Naik JJ. Design, development, and evaluation of spray dried flurbiprofen loaded sustained release polymeric nanoparticles using QBD approach to manage inflammation. Dry Technol. 2023;41(15):2418-30.
26. Chaudhari SP, Kure NG, Nikam SA. Optimization of risperidone and quercetin solid lipid nanoparticles loaded nasal insitu gel by design expert and quality by design approach. J Pharm Innov. 2025;20(2):51.
27. Saha M, Saha DR, Ulhosna T, Sharker SM, Shohag MH, Islam MS, et al. QbD based development of resveratrol-loaded mucoadhesive lecithin/chitosan nanoparticles for prolonged ocular drug delivery. J Drug Deliv Sci Technol. 2021;63:102480.
28. Patel P, Thanki A, Kapoor DU, Prajapati BG. QbD decorated ellagic acid loaded polymeric nanoparticles: factors influencing desolvation method and preliminary evaluations. Nano-Struct Nano-Objects. 2024;40:101378.
29. Tan MI, Rahayu AK. Synthesis of chitosan-folic acid nanoparticles as a drug delivery system for propolis compounds. In: Multifaceted Protocols in Biotechnology, Volume 2. Springer; 2021. p. 145-59.
30. Siddiqui B, ur Rehman A, Gul R, Chaudhery I, Shah KU, Ahmed N. Folate decorated chitosan-chondroitin sulfate nanoparticles loaded hydrogel for targeting macrophages against rheumatoid arthritis. Carbohydr Polym. 2024;327:121683.
31. Taghipour-Sabzevar V, Sharifi T, Bagheri-Khoulenjani S, Goodarzi V, Kooshki H, Halabian R, et al. Targeted delivery of a short antimicrobial peptide against CD44-overexpressing tumor cells using hyaluronic acid-coated chitosan nanoparticles: an *in vitro* study. J Nanopart Res. 2020;22:1-16.
32. Kulkarni PV, Roney CA, Antich PP, Bonte FJ, Raghu AV, Aminabhavi TM, et al. Quinoline-n-butylcyanoacrylate-based nanoparticles for brain targeting for the diagnosis of Alzheimer's disease. Wiley Interdiscip Rev Nanomed Nanobiotechnol. 2010;2(1):35-47.
33. Nokhodi F, Nekoei M, Goodarzi MT. Hyaluronic acid-coated chitosan nanoparticles as targeted-carrier of tamoxifen against MCF7 and TMX-resistant MCF7 cells. J Mater Sci Mater Med. 2022;33(2):24.
34. Sun M, Wu J, Lian B, Cui J, Xu N, Xu Z, et al. Hyaluronic acid-modified liposomes co-encapsulating curcumin and mifepristone to enhance anti-breast cancer efficacy. J Drug Deliv Sci Technol. 2023;88:104956.
35. Farag MM, El-Sebaie W, Basalious EB, El-Gazayerly ON. Self-nanoemulsifying/self-assembled cubic nanoparticles lyophilized tablet: a novel biphasic release approach to enhance the bioavailability of a lipophilic drug. AAPS PharmSciTech. 2024;25(8):250.
36. Koirala S, Nepal P, Ghimire G, Basnet R, Rawat I, Dahal A, et al. Formulation and evaluation of mucoadhesive buccal tablets of aceclofenac. Heliyon. 2021;7(3):e06439.
37. Ismail A, El-Biyally E, Sakran W. An innovative approach for formulation of rutin tablets targeted for colon cancer treatment. AAPS PharmSciTech. 2023;24(2):68.
38. Vakar RM, Padhi S, Tiwari KS, Kinjal P. Development of colon targeting tablet of a JAK inhibitor to combat chronic ulcerative colitis: a novel approach for local drug delivery. Indian J Pharm Educ Res. 2021;55:s414-s27.
39. Prusty A, Patra A. Formulation and evaluation of ciprofloxacin colon targeted tablets by compression coating technique using guar gum and hydroxypropyl methylcellulose. J Res Pharm. 2022;26(6):1593-607.
40. Rasal P, Thul A, Shepal O, Pawar O, Sandhan N. Colon targeted drug delivery system: an overview on current approaches. Int J Sci Res Sci Technol. 2025;53(1).
41. Kudupudi V, Kakarparthy RS, Sarella P, Kolapalli V. Formulation development and characterization of vancomycin hydrochloride colon-targeted tablets using in-situ polyelectrolyte complexation technique. Int J Pharm Sci Nanotechnol. 2023;16(3):6533-45.
42. Vemula SK, Daravath B, Gummadi SB, Repka MJ. Formulation and development of flurbiprofen colon-specific eudragit coated matrix tablets: use of a novel crude banana peel powder as a time-dependent polymer. AAPS PharmSciTech. 2023;24(7):189.
43. Herdiana Y, Wathoni N, Shamsuddin S, Muchtaridi M. Drug release study of the chitosan-based nanoparticles. Heliyon. 2022;8(1):e08674.
44. Ijaz R, Ahmad Z, Khan MI, Usmani SJ, Sarwar HS, Sohail MF. Revolutionizing hypertension management: cutting-edge

microneedle patch infused with zinc oxide nanoparticles for advanced transdermal drug delivery. BioNanoScience. 2024;14(2):1397-409.
45. Hoang NH, Le Thanh T, Sangpueak R, Treekoon J, Saengchan C, Thepbandit W, et al. Chitosan nanoparticles-based ionic gelation method: a promising candidate for plant disease management. Polymers (Basel). 2022;14(4):662.
46. Parvathaneni V, Shukla SK, Gupta V. Development and characterization of folic acid-conjugated amodiaquine-loaded nanoparticles-efficacy in cancer treatment. Pharmaceutics. 2023;15(3):1001.
47. Sarnaik S, Ahmed H, Hussain N, Kundu S, Sahu BD, Alexander A. Folic acid-chitosan conjugated mesoporous silica nanoparticles for enhanced piceatannol uptake in MCF-7 breast cancer cells. ACS Omega. 2025. doi:10.1021/acsomega.5c05302.
48. Ghose D, Patra CN, Kumar BVVR, Swain S, Jena BR, Choudhury P, et al. QbD-based formulation optimization and characterization of polymeric nanoparticles of cinacalcet hydrochloride with improved biopharmaceutical attributes. Turk J Pharm Sci. 2021;18(4):452-64.
49. Türkeş E, Açıkel YS. Folic acid-conjugated cancer drug curcumin-loaded albumin nanoparticles: investigation of curcumin release kinetics. J Drug Deliv Sci Technol. 2024;91:105178.
50. Nunthanid J, Huanbutta K, Luangtana-Anan M, Sriamornsak P, Limmatvapirat S, Puttipipatkhachorn S, et al. Development of time-, pH-, and enzyme-controlled colonic drug delivery using spray-dried chitosan acetate and hydroxypropyl methylcellulose. Eur J Pharm Biopharm. 2008;68(2):253-9.
51. Huanbutta K, Luangtana-Anan M, Sriamornsak P, Limmatvapirat S, Puttipipatkhachorn S, Nunthanid J, et al. Factors affecting preparations of chitosan microcapsules for colonic drug delivery. J Met Mater Miner. 2008;18(2):79-83.
52. Huanbutta K, Sriamornsak P, Luangtana-Anan M, Limmatvapirat S, Puttipipatkhachorn S, Lim L-Y, et al. Application of multiple stepwise spinning disk processing for the synthesis of poly(methyl acrylates)-coated chitosan-diclofenac sodium nanoparticles for colonic drug delivery. Eur J Pharm Sci. 2013;50(3-4):303-11.
53. Nunthanid J, Luangtana-Anan M, Sriamornsak P, Limmatvapirat S, Huanbutta K, Puttipipatkhachorn S, et al. Use of spray-dried chitosan acetate and ethylcellulose as compression coats for colonic drug delivery: effect of swelling on triggering *in vitro* drug release. Eur J Pharm Biopharm. 2009;71(2):356-61.